Current Opinion in Solid State & Materials Science xxx (xxxx) xxxx

Contents lists available at ScienceDirect

Current Opinion in Solid State & Materials Science

journal homepage: www.elsevier.com/locate/cossms

Current understanding and emerging applications of 3D crumpling mediated 2D material-liquid interactions

Peter Snapp[a,1], Mohammad Heiranian[a,1], Michael Taeyoung Hwang[b,1], Rashid Bashir[b,c,*], Narayana R. Aluru[a,*], SungWoo Nam[a,*]

[a] Department of Mechanical Science and Engineering, University of Illinois at Urbana-Champaign, Urbana, IL 61801, USA
[b] Holonyak Micro and Nanotechnology Laboratory, University of Illinois at Urbana-Champaign, Urbana, IL 61801, USA
[c] Department of Bioengineering, University of Illinois at Urbana-Champaign, Urbana, IL 61801, USA

ARTICLE INFO

Keywords:
2D materials
Graphene
Texturing
Wrinkling
Corrugation
Surface properties
Wettability
Electrical double layer
Biosensing
Templating

ABSTRACT

Three dimensional (3D) crumpling of two dimensional (2D) materials provides new opportunities to modulate mechanical, optical, surface, and chemical properties. However, investigation of the effect of 3D crumpling on 2D material liquid interaction has been limited. In this perspective, we will review crumple/texture induced heterogeneous surface properties including chemical modification, energy corrugation, and electronic structure perturbation which may modulate fluid interaction. We will then describe simulations of fluid interaction in systems resembling 3D textured 2D materials, principally nanotubes, which have begun to substantiate perturbations to fluid structure driven by texture induced modification of the 2D material surface. Furthermore, we will detail current experimental understanding of how texture induced modulation of interactions with pure solvent affect macroscale wetting characteristics including textured driven transitions in water contact from Wentzel to Cassie Baxter states. Following this discussion of how texturing affects the interaction of 2D materials with pure solvent, we will detail cutting edge explorations of how texturing modifies interaction with ions and other chemical species dispersed in solvent phases. Particular focus will be placed on recent simulations of aqueous phase molecular interaction with crumpled 2D materials which show that crumpling increases the thickness of the electrical double layer (EDL) formed near a 2D material surface. This increased EDL thickness has allowed for the development of biomolecule sensors with gigantic sensitivity and the monitoring and templating of cells including neurons and myotubes. Sill, considerable work is needed to elucidate the effect of different crumpling geometries on the local properties of the full range of 2D materials, how these variation in local properties perturb fluid structure and molecular interaction, and how these tuned interactions enable diverse opportunities such as sensing, energy storage, and control of biological interaction.

1. Introduction

Two Dimensional (2D) materials have commanded the attention of the broad scientific community for over a decade. For instance, graphene, a semi-metallic, 2D form of carbon and the best known 2D material, is the thinnest and strongest known material, demonstrates ultrahigh electrical mobility and thermal conductivity, and is molecularly impermeable [1]. The family of 2D materials has grown to include insulators like hexagonal boron nitride (h-BN), semiconductors like transition metal dichalcogenides (TMDs), metals like 2D vanadium oxides, and many more [2]. Despite this great diversity, all 2D materials are characterized by atomic scale thinness which results in unique interfacial interactions. Transitioning focus back to graphene which possesses surface behaviors representative of the broad family of 2D materials, one can begin to understand the complex interactions occurring at the surface of a 2D material. Graphene demonstrates long range π conjugation and interacts with weakly adsorbed molecules by donating or accepting charge carriers resulting in modulation of carrier concentration [3]. This π-π interaction and electron donation result in complex behaviors including variations in solubility and catalysis that can be modulated by doping and defect engineering [4]. The ability to actively tune surface interactions using 2D materials offers broad opportunities for interfacial engineering, particularly in controlling interactions at the solid–liquid interface.

* Corresponding authors.
E-mail addresses: rbashir@illinois.edu (R. Bashir), aluru@illinois.edu (N.R. Aluru), swnam@illinois.edu (S. Nam).
[1] These authors contributed equally to this work.

https://doi.org/10.1016/j.cossms.2020.100836
Received 20 April 2020; Accepted 19 June 2020

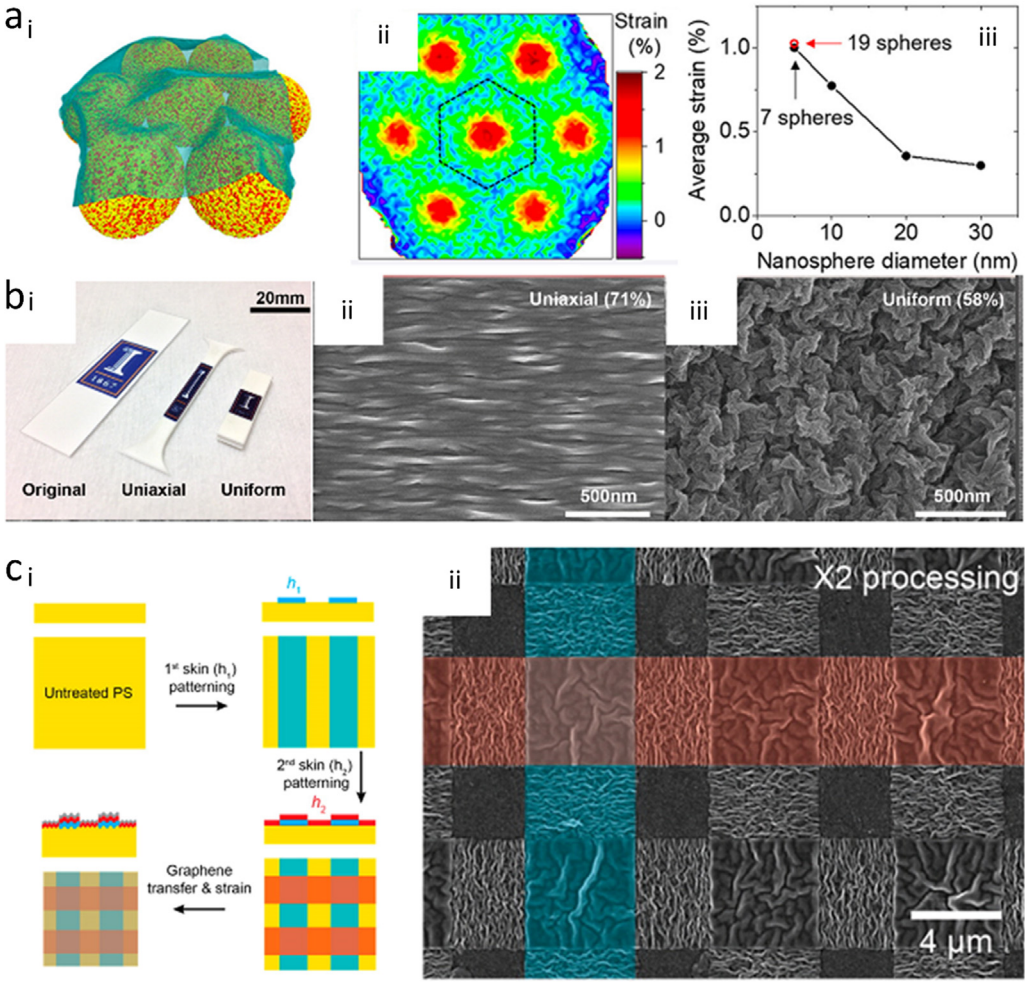

Fig. 1. Various texturing geometries and their key characteristics. (**a**) Conformal wrinkles: (i) Conformally wrinkled graphene produced by transfer over seven 20 nm diameter nanospheres (NS). (ii) profiles of areal strain for conformally wrinkled graphene on 5 nm nanospheres. (iii) Average graphene areal strain above the central sphere (dashed hexagon in (ii)), vs. NS diameter. Black dots correspond to data collected from graphene on an assembly of seven NSs, red circles corresponds to graphene on an assembly of 19 NSs [Reproduced with permission from Ref. [22] Copyright (2018) American Chemical Society]. (**b**) Delaminated crumples: (i) Photograph illustrating the original untreated sample of graphene on polystyrene (original, left) versus samples subjected to various texturing schemes of uniaxial strain (middle) and uniform/equi-biaxial strain (right). High-magnification scanning electron microscopy (SEM) reveals the unique resultant graphene crumple morphologies due to uniaxial (71%) (ii) and equi-biaxial/uniform (58%) (iii) strains, respectively [Reproduced with Permission from Ref. [24] Copyright (2015) American Chemical Society]. (**c**) Hierarchical wrinkle structures: (i) Utilization of an iterative skin-patterning processes (double masking) to fabricate hierarchical graphene wrinkles. (ii) SEM images showing hierarchically textured graphene on the patterned skin layers using double masking [Reproduced with permission from Ref. [23] Copyright (2016) American Chemical Society]. (For interpretation of the references to color in this figure legend, the reader is referred to the web version of this article.)

The liquid – 2D material interface offers various options for control and tuning. Wettability, the most basic interaction between a fluid and a surface, of 2D materials is highly complex due to perturbation from the environment [5]. For instance, planar, unmodified graphene is widely considered hydrophilic with freshly prepared graphite under ultrahigh vacuum and graphene exposed to air for less than one minute demonstrating hydrophilicity (water contact angle (WCA) $< 90^{\circ}$) [6]. This inherent hydrophilicity is reflected in theoretical studies with WCAs predicted using molecular dynamics (MD) simulations and ab initio calculations consistently showing values less than 90° regardless of the number of layers simulated [7]. However, this inherent hydrophilicity is easily perturbed by the environment which the 2D material is exposed to. In particular, the extreme thinness of 2D materials results in wetting translucency to the substrate. For example, 2D materials with fluid interactions dominated by van der Waals forces including graphene, molybdenum disulfide (MoS_2), and tungsten disulfide (WS_2), develop non-negligible polar natures after transfer to strongly polar h-BN surfaces [8]. Similarly, physisorption of airborne hydrocarbons profoundly changes the wettability of graphene, causing a transition to hydrophobic behavior over time [9]. Perturbation of surface properties extends beyond wettability, for instance, the formation of an electrical double layer (EDL) above graphene shows a distinct dependence on the substrate, with EDL capacitance declining with increasing hydrophobicity of the substrate [10]. Another driving factor modifying 2D material properties are three-dimensional (3D), out-of-plane surface instabilities which modify interaction directly through structure and by perturbing the properties of the 2D material through heterogenous strain.

Crumpling/texturing 2D materials to adopt an out-of-plane geometry has emerged as a key technique to modify the properties of 2D materials. Crumpling offers a simple route to tune 2D material interactions that can be reversed and produces heterogeneous surfaces [11]. For instance, the interlayer shear modulus and shear strength of interacting graphene sheets are easily increased with the introduction of out-of-plane wrinkles which induce geometrical locking effects between the interacting layers [12]. Similarly, crumpling induces areal densification of graphene which increases optical absorbance and is reversible by application of strain, allowing for the development of tunable, crumpled graphene photodetectors [13]. Crumpling also offers an interesting route to create 2D material heterostructures with induction of a sinusoidal wrinkle structure predicted to induce controllable phase transitions in TMDs resulting in alternating domains of semiconducting 2H phase and metallic T phase [14]. Still, direct exploration of the effect of crumpling on the surface interactions of 2D materials at the liquid interface has been quite limited.

While it is well understood that 3D surface features influence wettability [15] and electrostatic interaction at the interface between liquids and solids [16], the influence of 3D crumpling on 2D material liquid interaction has been explored only superficially. In the case of wettability, it is understood that crumpling 2D materials causes a transition from Wentzel to Cassie Baxter states provoking transition from hydrophilicity to hydrophobicity [17]. However, texturing 2D materials results in heterogeneous modification of surface properties including local variations in chemical functionalization [18], friction

[19], and doping [20] which are not observed with patterned bulk materials and are likely to modify interaction with an interacting solvent in a complex manner, meriting further exploration. Similarly, corrugations on 2D materials have allowed for the realization of spatially defined chemistry [18], but the detailed structure of the EDL over textured 2D materials, which modulates electrochemical interaction, is only just being investigated. Given the implications of wettability and EDL structure on the use of nanotextured 2D materials for sensing and tailored biological interactions [16], developing a full understanding of the effect of texturing on the 2D material-liquid interface is of significant importance.

In this perspective, we will review known effects that perturb the wettability of 2D materials, identify how these perturbations are influenced by texturing, and propose questions on textured 2D material – liquid interactions yet to be addressed. We will then describe emerging progress on understanding EDL structure above textured 2D materials and the implications of EDL structure modification on interaction with ions and other chemical species dispersed in solvent phases. Finally, applications enabled by texture driven tunable wettability and EDL structure will be reviewed, with particular attention payed to emerging applications in biological sensing and modulation of cell-textured 2D material interactions.

2. Survey of 2D material crumpling approaches

Before delving into a discussion of the effects of texturing on 2D material-liquid interactions, it is important to discuss the varying 2D material texture geometries available, each having distinct interactions with fluid. Texturing geometries can be subdivided into three categories: conformal wrinkles, delaminated crumples, and hierarchical topographies. Conformal wrinkles (Fig. 1a) maintain continuous contact with their supporting substrate and can be produced by direct growth of 2D materials on textured substrates [21], deposition/transfer of sheets of 2D material onto texturing templates (Fig. 1a(i)) [22], or transfer of 2D materials to pre-strained substrates overcoated with skin layers which adhere strongly to deposited 2D material layers [23]. Conformally wrinkled 2D materials experience non-uniform strain which peak at the wrinkle apex (Fig. 1a(ii)), and, given constant material thickness and feature aspect ratio, increases as feature size decreases (Fig. 1a(iii)) [22]. Non-uniform strains perturb 2D materials electronic structure resulting in band structure manipulation [22] and orbital hybridization [18] which might modify interaction with liquids. In contrast, delaminated crumples (Fig. 1b) form voids beneath the peaks of the crumples and are readily produced by contraction of 2D layers which are weakly adhered to substrates which allow 2D film delamination (Fig. 1b(i–iii)) [24]. The void beneath the delaminated crumples results in collapse, forming dense high aspect ratio features (Fig. 1b(ii–iii)) which change water droplet contact from the conformal Wenzel state to the trapped air Cassie-Baxter state [17]. Conformal wrinkles and delaminated crumples can be realized simultaneously using hierarchical topographies (Fig. 1c) which can be produced by sequential mechanical deformation [25], varying the number of 2D material/skin layers crumpled (Fig. 1c(i)) [23], or integration of graphene over swollen templates [26]. The precise control of structure afforded by hierarchical texturing (Fig. 1c(ii)) could allow control of liquid − 2D material interaction for tunable wettability and catalysis [27]. Given the diversity of texturing geometries available, each with distinct effects on 2D material properties, detailed exploration of the behavior of liquids interacting with these structures is needed. This exploration of variation in textured 2D material – liquid interaction driven by different texturing geometries will enable diverse applications including surface treatments, sensing, and controlled biological interaction.

3. Effect of crumpling on 2D material – liquid phase interactions

3.1. Texture-driven modification of 2D material surface properties and liquid interaction

At the most basic level texturing 2D materials produces structures simulating large scale surface roughness and out of plane defects [17]. It is well known that structural defects modulate wettability of the typically flat surfaces of both 2D and bulk materials. For instance, the formation of out-of-plane structures such as vertical graphene networks, renders graphene hydrophobic by trapping air at the liquid – 2D material interface [28]. However, in our view, richer opportunities for tuning wetting are enabled by the complex, heterogeneous modification of 2D material surface properties resulting from crumpling/texturing [11]. This spatially varying modulation of surface properties could result in complex perturbations to the behavior of liquids near a textured 2D material surface which will not be apparent on patterned bulk materials which maintain homogeneous surface properties. These modifications to water behavior over 2D materials can be predicted by examining how texturing or its analogs affect the surface properties of 2D materials and how these modified surface properties affect wettability and fluid interaction. The combined effects of these various influences on textured 2D material – fluid interaction could result in water behavior distinct from that over flat 2D materials and patterned bulk material surfaces.

First, texturing induced variations in the chemical activity of graphene [18] and similar 2D materials including MoS_2 [29] result in heterogeneous chemical decoration of flat 2D materials. For instance, delaminated graphene crumples demonstrate greater curvature than conformal wrinkles as indicated by atomic force microscopy (AFM) profiling (Fig. 2a(i)). This increased curvature enhances hybridization between the σ- and π-orbitals in wrinkled regions resulting in area selective fluorination as indicated by local variation in the ratio of the graphene's Raman G and 2D peaks (Fig. 2a(ii)) [18]. The effect of this texture driven variation in chemical activity is analogous to chemical functionalization/modification across the 2D material surface. Chemical decoration/modification is the most basic perturber of 2D material wettability [30]. However, modulation of wettability becomes more complex when the contamination or surface modification is heterogeneous across the surface. Textured 2D materials demonstrate distinctive regions of chemical activity distributed laterally across the surface [18] resulting in wettability in between that of unstrained and homogeneously strained graphene, similar to the intermediate wettability of hyrofluorinated graphene between hydrogenated and fluorinated graphene (Fig. 2b) [31]. However, depending on the degree of texturing and the specific texture geometry, the distribution of functional groups on textured graphene will differ significantly from the atom scale distribution of functional groups on functionalized graphene, influencing the local contact state of liquids and changing contact angle.

In addition to variations in chemical activity, texturing 2D materials creates corrugations in potential energy and modulates frictional interaction. Out-of-plane corrugations on graphene epitaxially grown on Ru(0 0 0 1) directly obstruct smooth sliding and result in local variations in potential energy across a graphene surface arising from enhanced interfacial electronic interaction at corrugated areas. Similar variation in potential energy is observed for graphene sliding over a textured gold surface (Fig. 3a(i)) resulting in a spatially varying graphene-gold interaction potential (Fig. 3a(ii)) [32].These obstructions to sliding and variation in potential energy result in stick slip frictional behavior [33]. Modified frictional behavior influences 2D material fluid interaction, modulating the slippage of molecules across a surface with implications for lubrication, and energy storage [19]. Slippage of water over a 2D material surface is influenced by periodic variations in potential energy across a surface, *i.e.* energy corrugation, which is most apparent when comparing graphene and 2D hexagonal boron nitride

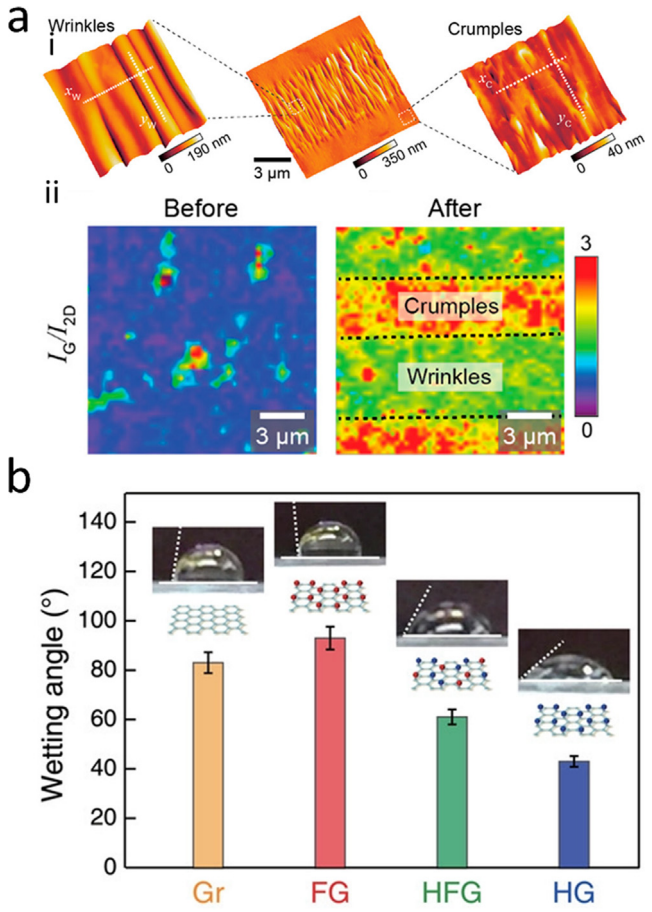

Fig. 2. Heterogeneous chemical decoration of graphene facilitated by texturing and potential effects on fluid interaction. (**a**) Selective fluorination of graphene using 1D wrinkles and crumples. (i) AFM of wrinkled and crumpled graphene regions. The zoomed-in images for wrinkles and crumples at the right and left of (i) represent 1 × 1 μm^2 areas. (ii) Raman mapping of graphene I_G/I_{2D} ratios before (left) and after (right) fluorination [Reproduced with permission from Ref. [18] Copyright (2019) American Chemical Society]. (**b**) Contact angles of water droplets on graphene (Gr), fluorinated Gr (FG), hydrogenated Gr (HG), and hydrofluorinated Gr (HFG) surfaces. Insets are images of representative droplets on each surface [Modified after (Zande et al.) [31]. (© 2019, John Wiley and Sons) (license: https://creativecommons.org/licenses/by/3.0/legalcode)].

(hBN). hBN exhibits a 3 fold increase in liquid friction compared to graphene (Fig. 3b(i)). This drastic difference in water slippage is attributed to a larger corrugation of the hBN energy landscape (21 meV) compared to graphene (13 meV) (Fig. 3b(ii[1,2])). On graphene, water molecules weakly prefer absorption onto the center of the graphene hexagon over positioning above carbon atoms (Fig. 3b(ii[3,4])) while on hBN water strongly prefers positioning over nitrogen atoms and avoids positioning over boron atoms (Fig. 3b(ii[5,6])) resulting in enhanced energy corrugation [34]. Increases in fluid friction over hBN is consistent among polar solvents with ethylene glycol exhibiting higher friction as a result of enhanced electrostatic interaction with the corrugated energy landscape of hBN while non-polar diiodomethane demonstrates reduced friction as a result of weak electrostatic interaction [35]. Texturing 2D materials could have the combined effect of directly obstructing slippage of any liquid by introducing physical barriers while also creating a corrugated potential energy landscape, as was observed for corrugated graphene grown on Ru(0 0 0 1) [33], resulting in distinct frictional interaction with polar and non-polar solvents.

Corrugation not only creates out-of-plane structures but also induces strains [22] which modify the local electronic properties of 2D materials. Homogeneous strain applied to a single layer graphene sheet alters band structure, resulting in changes to the Fermi level of graphene (Fig. 4a) [36,37] which has the potential to influence interaction with liquid as changes in doping level are known to drive changes in WCA (Fig. 4b(i)) [20]. In a similar manner, homogeneous, mechanical strain increases graphene's reaction rate with functionalizing aryl diazonium molecules by a factor of 10, enabling increased functionalization with p- and n-type dopants which further modifies charge carrier concentration [38]. This texture driven extrinsic doping has the potential to further tune wettability and adhesion by increasing hydrophilicity which has been observed in both n- and p-type subsurface doped graphene (Fig. 4b(ii)) [20]. Combining the heterogeneous strain driven (Fig. 1a(i)) band structure modulation and extrinsic doping effects of texturing with electronic structure induced modulation of the wettability could result in complex modulation of wetting over a textured 2D material surface.

3.2. Influence of crumpling on wetting and open questions

These predicted influences of corrugation on 2D material – fluid interaction have been partially confirmed by experiment and simulation. Graphene/carbon nanotube (CNT) films, which simulate conformal wrinkles, exhibited surface hydrophobic properties including increased WCA and reduced slip angle which resulted from predicted modified water contact and were controllable by altering the film structure (Fig. 5a) [39]. Explicit perturbation of water structure near concave and convex regions of a conformally wrinkled graphene film can be inferred from the structure of water inside (concave) and outside (convex) carbon nanotubes. Outside of tubes, water molecules move to low-energy potential wells formed near the hexagonal carbon surface leading to increased density and nonuniform molecular distribution at the exterior carbon surface that does not vary with tube diameter. In contrast, inside tubes, water behavior strongly depends on tube diameter, with water in large (> 10 nm diameter) tubes behaving like water outside tubes while water in small (< 10 nm diameter tubes) demonstrates reduced water density resulting from the curved surface pinching the low-energy potential wells, pushing water molecules away from the carbon surface. This reduction in water density inside tubes become more pronounced as the tube diameter is further reduced (Fig. 5b) [40].

Explicitly discussing textured graphene, buckle delaminated graphene mimics superhydrophobic leaves [17] and multilayer graphene showing complex, out-of-plane textures (Fig. 5c(i)) demonstrated systematic increases in hydrophobicity with successive generations of texturing, eventually demonstrating superhydrophobicity after three-generations of extreme compression (Fig. 5c(ii)) [25]. This effect is present across multiple 2D materials with hierarchically textured nanoflower MoS_2 demonstrating a hydrophobic WCA which reduces reversibly when the textured structure is flattened by application of strain (Fig. 5d(i)), and is stable over thousands of cycles of stretch and release (Fig. 5d(ii)) [27].

In spite of this progress, more work is needed to fully understand the detailed mechanisms driving textured 2D material – fluid interaction enabling diverse applications. Understanding variation in wettability arising from texture driven heterogeneity in chemical reactivity will inform the use of textured 2D materials as substrates for fluid phase catalysis [27]. Similarly, understanding the frictional interaction between a fluid and a textured 2D material will establish the utility of crumpled 2D materials in microfluidics applications and as lubricating surfaces [19]. Furthermore, local variation in wettability driven by texture associated heterogeneous strain will enable the use of textured materials as surface coating and barrier materials as well as sensing and templating platforms [16,20]. Modified liquid behavior can be probed experimentally at several length scales, using macroscale WCA measurements to determine general wettability, mesoscale Raman and energy dispersive X-Ray spectroscopy [18] to probe local chemical

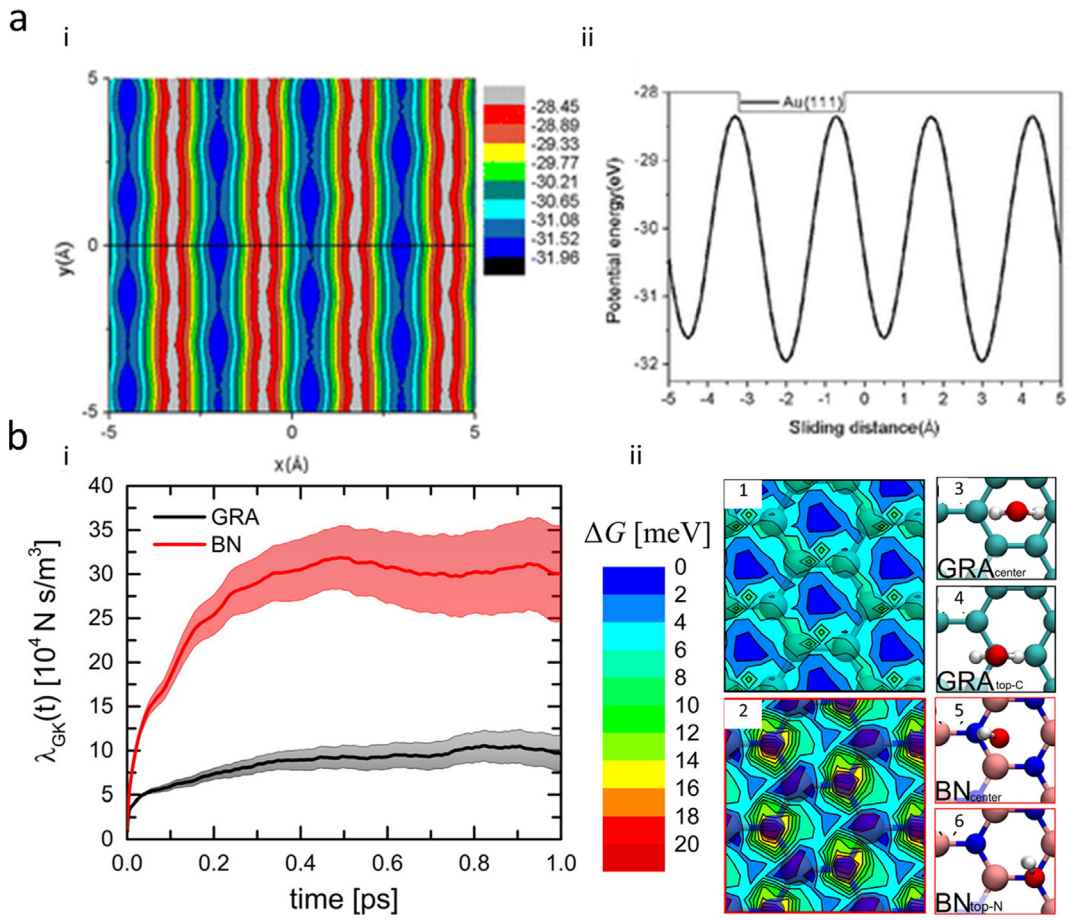

Fig. 3. Texture driven modification of 2D material frictional behavior and its effect on fluid interaction. (**a**) Potential energy corrugation driven by corrugation of sliding graphene on an Au(1 1 1). (i) contour maps of the potential energy for the Au(1 1 1) surface with an adopted 5.8 nm square graphene flake, the potential energy is reported in eV. (ii) graphene-gold interaction potential energy along the sliding path is indicated by the black line in (i) [Modified after (Zhu et al.) [32]. (© 2018, SpringerNature) (license: https://creativecommons.org/licenses/by/4.0/legalcode)]. (**b**) Differences in slippage of water over graphene and hBN resulting from differences in energy corrugation. (i) Comparison between the Green–Kubo estimate of the friction coefficient of liquid water on graphene and on hBN. Uncertainties obtained by performing a block average are given by the shaded areas. The friction coefficient, λ, is given by the plateau. λ increases considerably on hBN. (ii) Free energy profile of water within the contact layer of the liquid projected onto the (1) graphene and (2) hBN primitive unit cells. A larger corrugation in free energy is present on hBN as well as minor differences in topography. Transparent graphene and hBN sheets are superimposed on the contour plots. (3) Most (3) and least (4) stable configuration for water molecule adsorbed on graphene. Most (5) and least (6) stable configuration for a water molecule adsorbed on hBN. Only a small part of the unit cells used for the monomer adsorption calculations is shown in panels (3) to (6) [Reproduced with permission from Ref. [34]. Copyright (2014) American Chemical Society]. (For interpretation of the references to color in this figure legend, the reader is referred to the web version of this article.)

modification, and nanoscale aqueous phase AFM [19] and scanning tunneling microscopy [40] techniques to map variations in surface energy and fluid structure. Experimental work can then be combined with large scale MD simulations [41] of liquid surface interaction informed by first principle calculations and ab initio/density functional theory (DFT) simulations which elucidate atom scale fluid interactions to confirm the mechanisms driving modified fluid interaction. In all cases exploration of fluid interaction involves correlating macroscale measurements of wetting behavior with local measurements of liquid molecule behavior. Therefore, a pre-requisite for full characterization of textured 2D material systems is the development of mesoscale simulation methods which can bridge molecular scale calculations with continuum simulations. Mesoscale simulation will capture the full effect of texturing in a single simulation that can be compared to macroscale experimental observations forming a cohesive picture of liquid – textured 2D material interaction.

4. Effect of crumpling 2D materials on electrical double layer formation

Controlling liquid behavior over textured 2D materials has the further effect of modulating interaction between ions and molecules in solution, motivating recent exploration of the use of textured 2D materials to control interfacial chemical interaction. These interactions are of particular interest because 2D materials can be used as electrodes for signal detection or as semiconductors in field-effect transistors (FETs) in solution [42-44]. In solution-based FETs, an EDL, consisting of a layer of counter-ions adsorbed onto a charged surface due to the interaction of counter-ions with the surface atoms and a second layer of co-ions attracted to the first layer [10], is formed above the channel. The electrolyte layer acts as an insulator between the semiconductor and the gate electrode in the solution [45], screening the charge of target molecules outside the layer, adversely affecting the molecule detection sensitivity of FETs [46-48]. EDL thickness is characterized by the Debye screening length motivating explorations to reduce Debye length using different methods [46,49-54]. Gao *et al.* [51] increased the Debye length by functionalizing channels with porous polymers which spread EDL ions away from the channel surface, preventing the formation of highly concentrated, thin EDLs and allowing ions and biomolecules to permeate through. High frequency AC methods [46,52-54] have also been used to disrupt the EDL formation and reduce the electrostatic screening, however, measuring the output signal and applying high

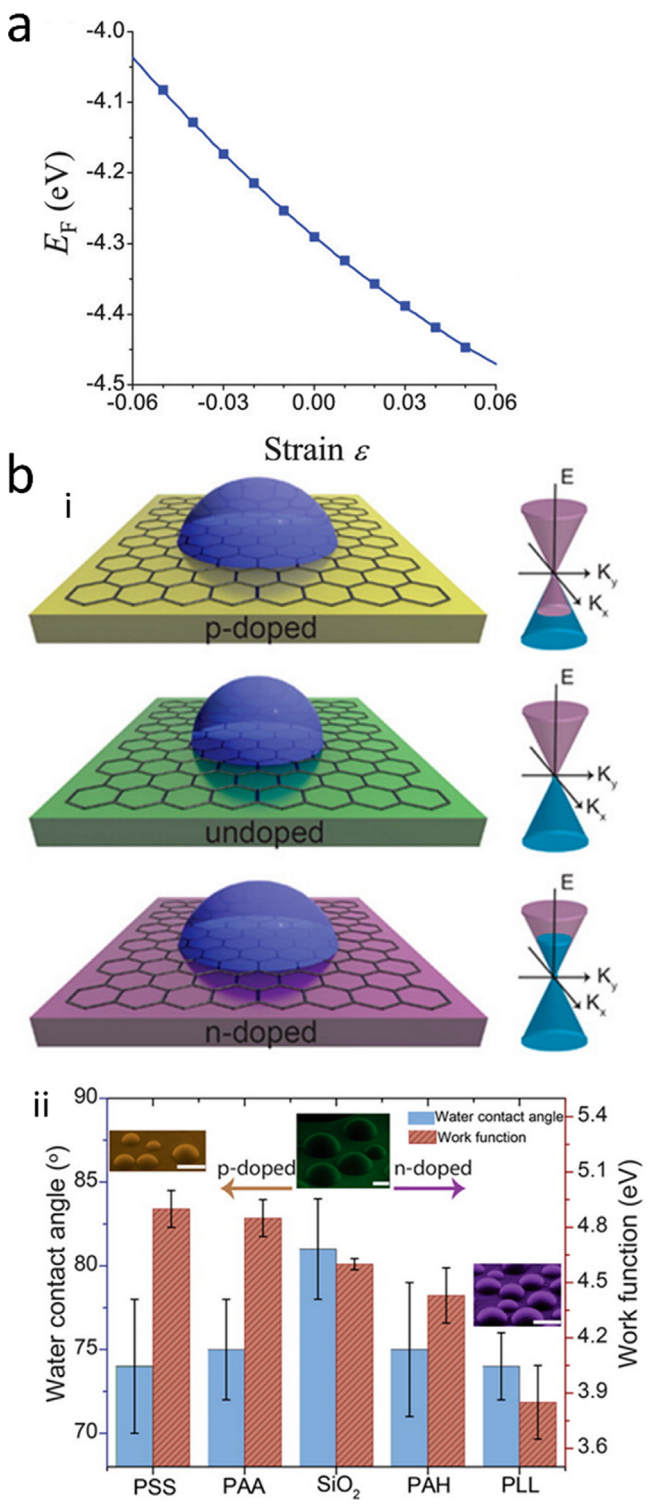

Fig. 4. Heterogeneous strain driven band structure modification of 2D materials and potential effects of water adhesion. (**a**) The variation of the Fermi (E_F) level of graphene with strain [Reproduced with permission from Ref. [36], with the permission of AIP Publishing.]. (**b**) Relationship between fermi-level and wettability. (i) Illustration of graphene wettability modulation achieved by shifting Fermi level via doping. (ii) Correlation between WCA (left axis) and work function (right axis) on polyelectrolyte-doped and undoped graphene samples. WCA was measured by environmental scanning electron microscopy (E-SEM) and work function was measured by scanning Kelvin probe microscopy. Graphene WCA decreases for both n-type and p-type doping. Insets correspond to E-SEM images of water droplets (false color, scale bars equal 10 μm) [Reproduced with permission from Ref. [20]. Copyright (2016) American Chemical Society.].

frequency voltage simultaneously require a complex operation [48]. One of the most effective routes to reduce screening effects is the use of small-size receptors [55,56] (*e.g.*, aptamers and monoclonal antibodies) to reduce the distance between the target molecule and the channel.

Surface morphology can also tune the structure of the EDL which, in return, changes the surface-EDL interfacial properties (*e.g.*, capacitance and electrostatic screening). Since strong electrostatic screening is detrimental to the sensitivity of FETs, the intrinsic curved nature of crumpled 2D materials can be exploited for fabrication of FETs with enhanced sensitivity. Shoorideh *et al.* [16], using the analytical Poisson-Boltzmann equations, has shown that charge screening decreases for concave surfaces. M. T. Hwang *et al.* recently extended this work, offering the first exploration of the influence of texturing 2D materials on EDL structures [57]. All-atom MD simulations were used to compare the EDL structures near concave and convex graphene surfaces with that of a flat graphene sheet. In Fig. 6, where the molar concentration of ions is shown near charged flat and crumpled graphene surfaces, the structural properties of the EDL next to a curved graphene surface differs from that of an ideally flat graphene. Most importantly, a longer EDL is formed near the concave surface due to the confinement. Biomolecules adsorbed onto the concave surface are shown [57] to exclude ions from the surface, spreading the EDL further away from the concave surface. Therefore, concavity of the surface results in more exposure of biomolecule charges without being screened by ions. The promise of possible reduced screening in crumpled graphene can potentially alleviate the EDL screening and improve the sensitivity of future detection devices as discussed later in this perspective.

Modified EDL screening also has implications for energy storage. EDL capacitors are supercapacitors that work based on the adsorption of ions to the electrode surface (Fig. 7) [58]. Compared to traditional batteries, supercapacitors can be charged and discharged much faster, in seconds, with a longer cycle life ($> 10^5$ charge/discharge cycles) [59-61], however, EDL supercapacitors lack high energy densities [59-63]. Energy density can be increased by maximizing the interfacial area where ions are accumulated. Single-layer graphene, having a high theoretical surface area of 2630 m^2/g, is a good candidate due to high surface area, superior electrical properties, and chemical inertness [60,62]. Hengxing *et al.* [64] showed that single-layer graphene has higher capacitance than multi-layer graphene because of stronger correlations between EDL ions and the π-band electron Fermi liquid in single-layer graphene. Kwon *et al.* [10] further showed that using a hydrophilic substrate to support single-layer graphene increases the EDL capacitance further by forming a thinner EDL at the graphene interface while hydrophobic substrates disturb EDL formation, reducing capacitance (Fig. 7a–c). Still, graphene-based supercapacitors suffer from low energy densities due to the low density of states at the Fermi level which leads to small quantum capacitance [62-65].The total interfacial capacitance is given by summing graphene quantum capacitance and EDL capacitance in series ($C_T^{-1} = C_Q^{-1} + C_{EDL}^{-1}$ where C_T, C_Q and C_{EDL} are the total, quantum and EDL capacitances, respectively) and is dominated by the small quantum capacitance [65]. Quantum capacitance can be tuned by modifying the electronic properties of graphene through molecular doping, point defects, and deformation or morphological modification [66-71]. Nitrogen doping can enhance the quantum capacitance of graphene by changing carrier charge density of graphene [66,70,71]. Redox active molecules have also been used to increase the capacitance of graphene [68,69]. Wood *et al.* [71] achieved enhanced quantum capacitance by introducing different types of point defects. Most relevantly, Wood *et al.* [71] investigated the effect of straining and crumpling of graphene on the quantum capacitance. Since tensile strain increases the capacitance as the surface area increases, larger enhancement is achieved by crumpling with enhancement scaling inversely the crumple wavelength (Fig. 7d). Crumpling weakens π-bonds with small π-π* splitting which, in return, leads to a higher density of states at the Fermi level increasing the quantum capacitance [71] (Fig. 7e–f). These promising results with crumpled graphene, pave

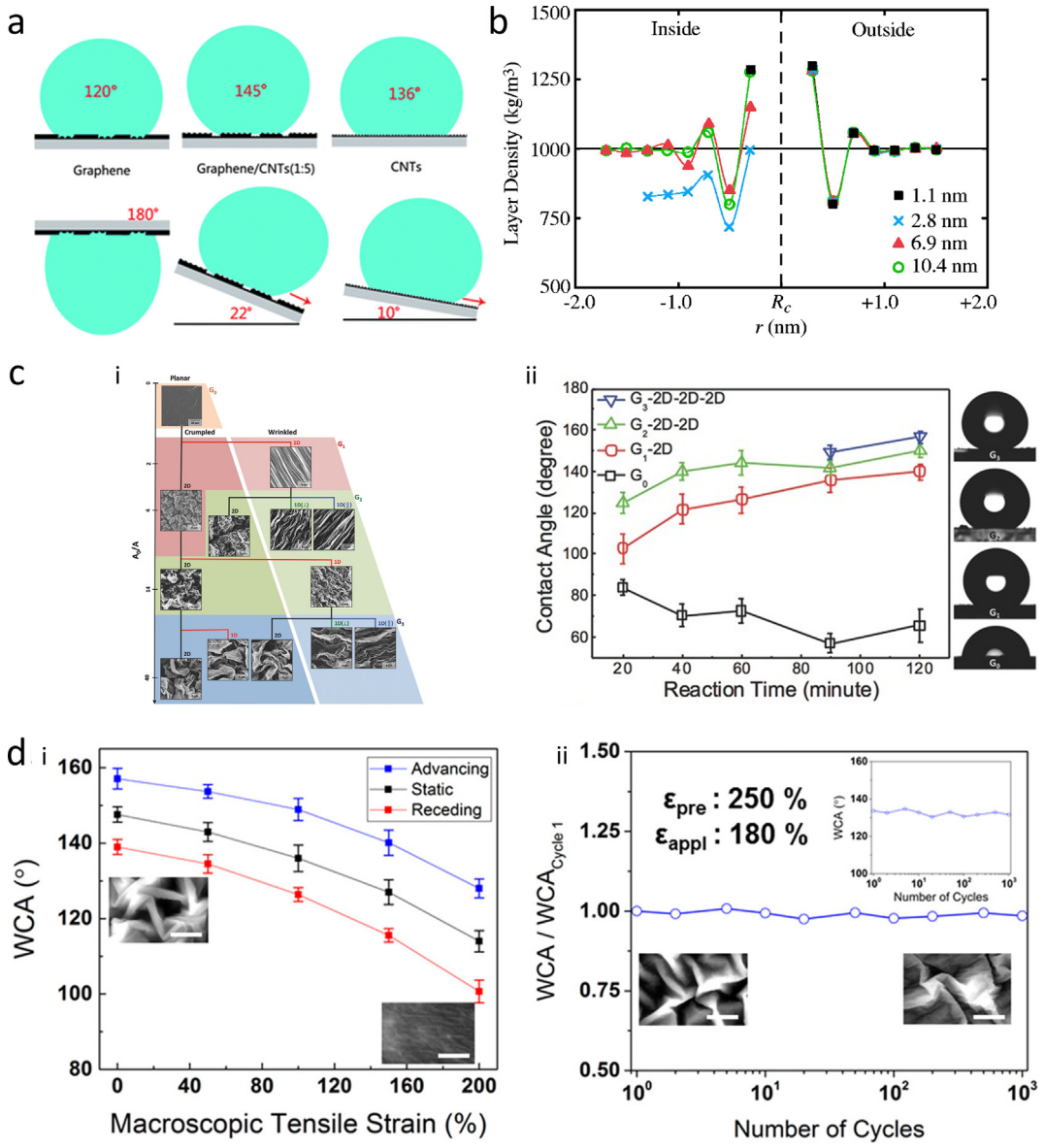

Fig. 5. Explicit effect of texturing on wetting behavior of 2D materials. (**a**) Schematics of hydrophobic and anti-adhesive mechanism of pure graphene films, graphene/CNTs film with a 1:5 mass ratio, and pure CNT films [Used with permission of Royal Society of Chemistry from Ref. [39]; permission conveyed through Copyright Clearance Center, Inc.]. (**b**) Density of water inside and outside CNTs for different radii. The density profile of water outside CNTs is invariant with diameter and the same as that near a flat graphene sheet. The density profile inside the CNTs depends on tube diameter [Reprinted from Ref. [40], with the permission of AIP Publishing.]. (**c**) Effect of delaminated crumpling on the wettability of graphene. (i) the genealogy of reduced graphene oxide (rGO) multi-generational structures from planar, G_0, coatings to multiscale, G_3, structures. A_0 is the area of initial planar film; A is the area of multigenerational rGO film. Scale bar in the SEM of G_0 coating is 10 μm, and scale bars in G_1, G_2, G_3 SEM images are all 4 μm. (ii) Static WCAs of hierarchical structures across various generations and the effect of hydrophobic functionalization reaction time on static WCA [[Modified after (Wong et al.) [25]. (© 2016, John Wiley and Sons) (license: https://creativecommons.org/licenses/by/3.0/legalcode)]. (**d**) Dynamic wettability of hierarchical, dual-scale MoS_2 as a function of stretching. (i) Wettability vs. biaxial tensile strain for crumpled nanoflower MoS_2 produced by transfer of nano-flower MoS_2 onto prestrained (200%) Ecoflex and releasing prestrain. Measurements were made simultaneously with application of biaxial tensile strain. Insets correspond to nanoflower MoS_2 at crumpled (left) and stretched (right) states. Scale bars equal 5 μm. (ii) Constancy of wettability during biaxial stretch and release (1000 cycles). Inset corresponds to SEM images of a 180% restretched sample after one (left) and 1000 (right) cycles. Scale bars equal 5 μm [Reprinted (adapted) with permission from Ref. [27]. Copyright (2017) American Chemical Society.].

the way for the realization of graphene supercapacitors with high energy densities. The effect of curvature on capacitance has been also studied utilizing a graphene functionalized with C60 buckyballs as curved surface electrodes, simulating conformally wrinkled graphene [72]. C60/graphene was shown to perform better compared to flat graphene with total capacitance enhanced 4 fold (see Fig. 7g) as a results of higher density of states at the Fermi level, increasing quantum capacitance, and absorption of more ions per unit area on the curved buckyball surface, increasing EDL capacitance.

5. Effect of 2D material crumpling on chemical and electrochemical reactions

While 2D materials have drawn attention for tuning ionic interaction, accessing the full potential of 2D materials is not possible without altering their chemistry [73]. Catalyzing electrochemical reactions (*e.g.*, oxygen reduction reaction (ORR) and hydrogen evolution reaction (HER)) by 2D materials can be enhanced by modifying the surface chemistry of 2D materials [74,75]. Chemical functionalization can be used for chemical modification [76]. However, functionalization of the

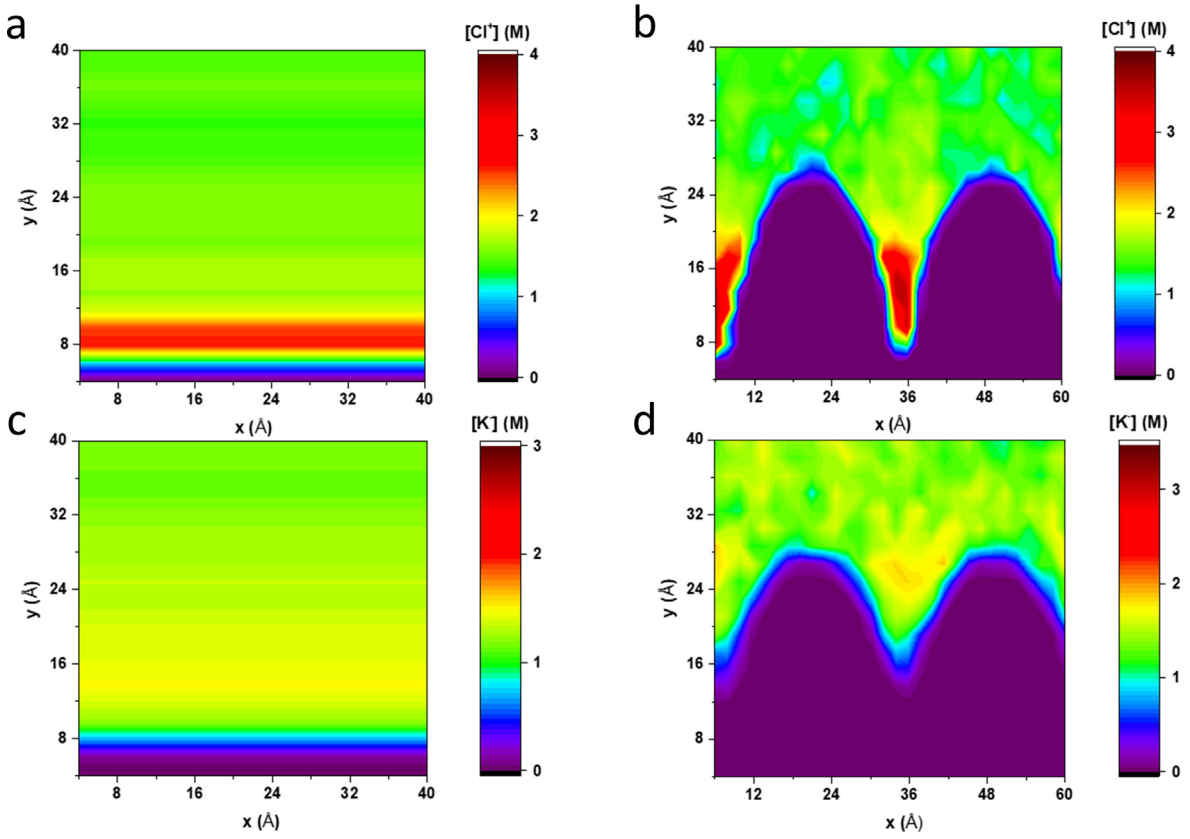

Fig. 6. Molar concentration map of sodium and chloride ions plotted for a flat (**a** & **c**) and a crumpled, charged sheet of graphene (**b** & **d**). Chloride, counter-ions are distributed over a longer distance from the graphene surface in concave regions of crumpled graphene (**b** & **d**) resulting in increased Debye length and enhanced charge detection sensitivity. [Modified after (Hwang et al.) [57]. (© 2020, SpringerNature) (license: https://creativecommons.org/licenses/by/4.0/legalcode)].

basal plane of graphene is difficult as π-conjugation leads to high energy barriers for reaction with functional groups [77]. Inducing local curvature by texturing results in hybridization of orbitals in graphene and increases its chemical reactivity with functionalizing molecules [18]. In addition to easing functionalization, texture induced enhancement of chemical reactivity enables 2D materials for use as liquid phase electrochemistry and catalysis platforms. DFT calculations predict texture induced enhancement of the catalytic activity of graphene, establishing that a minimum ratio of crumple height to radius of 0.07 is needed to enhance chemical reactivity of graphene [78] and that inducing a 2.0 nm radius of curvature reduces the energy barrier for hydrogen reduction by 15%[79]. Y. Qu *et al.* [74] experimentally investigated the effect of curvature on hydrogen evolution reaction of graphene, confirming that HER is abruptly enhanced on curved graphene subject to 10–30% compression as a result of Gibbs free energy increasing significantly upon crumpling (Fig. 8a–b). It is also likely crumpling graphene can be used to create platforms for oxygen reduction. Single-layer graphene draped over an underlayer of catalytic gold particles enhances the oxygen reduction reaction (Fig. 8c) which when probed using scanning electrochemical microscopy (Fig. 8d) manifests as increases in measured current which peaks at the center of the substrate (gold particles) [75]. While this enhancement is explained as an effect of the electrochemical transparency of ultrathin graphene [75], it is possible ORR and other electrochemical reactions catalyzed by 2D materials can be further improved by introducing curvature and altering the electronic properties of 2D materials, as was observed with HERs.

6. Emerging applications of crumpled 2D materials for biosensing and cellular templating

Modified fluid and electrochemical interactions enabled by texturing 2D materials offer promise for biological sensing and directing cellular growth. Biosensors capture target biomolecules, nucleic acids, proteins, carbohydrates, *etc.*, and transduce the reaction into recognizable signals. As target molecules are generally low in concentration, high sensitivity and specificity are required for effective biosensing. Electrochemical biosensors are particularly useful as they integrate probes, which generate signals from biological/chemical events, with electrical transducers which convert signals to easily quantified electrical information. Electrochemical biosensors can be categorized by their transduction methods which include capacitive, potentiometric, amperometric/voltammetric, conductometric, impedimetric, and FET sensors. FET sensors have received particular interest for biosensing as they are highly sensitive and are easily integrated into microarrays with other electronic components forming the basis for lab-on-a-chip systems. Many semiconducting materials have been tested for FET-biosensing including silicon [80], 1D carbon nanotubes [81], and Si nanowires [82]. 2D materials are attractive as active materials because they are easily fabricated uniformly over a large area with a single-atom thickness. Graphene is a promising material for FET-based biosensing because of its high carrier mobility, low intrinsic electrical noise, mechanical strength, and flexibility [83]. Graphene based FETs are ubiquitous in the literature as biomolecular sensing platforms targeting bacteria [84], glucose [85], protein [86], pH [87], and DNA [88,89] Incorporation of graphene in FET transducers remarkably improved sensing performance as a result of graphene's superior carrier transport and active surface area to volume ratio. For example, graphene FET-based biosensors were successfully able to detect proteins at

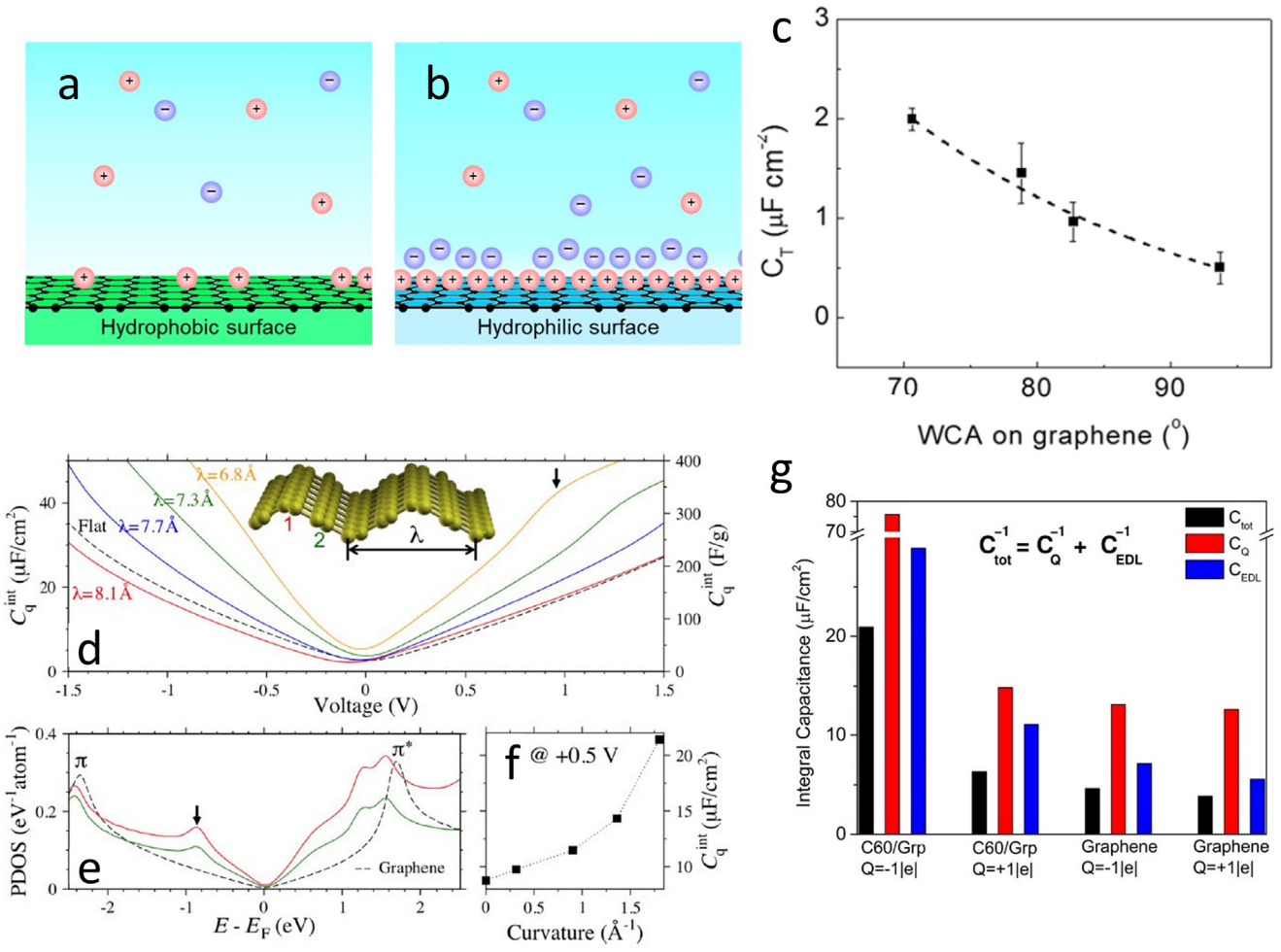

Fig. 7. (**a**) Illustrations of EDL formation on graphene supported on hydrophobic and hydrophilic substrates. It is hypothesized that EDL is disordered on graphene supported by (**a**) hydrophobic substrates relative to (**b**) hydrophilic substrates as a result of the influence of the substrate on the surface energy of graphene. Suppressed EDL formation over graphene on hydrophobic substrates leads to a decreased EDL capacitance. (**c**) Capacitance of graphene as a function of the WCA of the substrates where it decreases with hydrophobicity (higher contact angles) [Reprinted (adapted) with permission from Ref. [10]. Copyright (2019) American Chemical Society] (**d**) Theoretical area-specific integrated quantum capacitance C_q^{int} of graphene upon surface rippling induced by compressive stress. Results are for characteristic wrinkle wavelengths of, λ = 6.8, 7.3, 7.7, and 8.1 Å). (**e**) Partial density of states for rippled graphene (λ = 6.8 Å), projected onto carbon atoms at the ripple peak (red curve, site 1) and the inflection point (green curve, site 2). The dashed line corresponds to reference data for pristine graphene. (**f**) Dependence of C_q^{int} at +0.5 V on local curvature at the ripple peak [Reprinted (adapted) with permission from Ref. [71]. Copyright (2014) American Chemical Society.]. (**g**) Relative contribution of quantum and EDL capacitances to the total capacitance of the hybrid and graphene electrodes at different charges states. Higher capacitance in Graphene/C60 is due to the enhancement in both the EDL and the electrode (quantum capacitance). [Reprinted (adapted) with permission from Ref.[72]. Copyright (2018) American Chemical Society.] (For interpretation of the references to color in this figure legend, the reader is referred to the web version of this article.)

concentrations of 10 fM [90] and nucleic acids (DNA or RNA) at the 100 fM level [91]. However, many rare biotargets are not detectable within this range of limit of detection (LOD) without preprocessing such as purification, denaturation, or amplification, requiring additional lab-scale equipment and manpower. Given that the advantage of using FET-based biosensor is to create a cost- and time-efficient lab-on-a chip system, detection of unamplified/unprocessed nucleic acids or other biomarkers with extremely low concentration is necessary.

3D texturing of 2D graphene has emerged in bio-applications as it can provide even higher surface-to-volume ratio and greater mechanical flexibility than flat graphene. Roy *et al.* synthesized epitaxial graphene nanowall arrays and demonstrated simultaneous electrochemical detection of dopamine, uric acid and ascorbic acid at sensitivities orders of magnitude higher than comparable reports [92]. Similarly, Akhavan *et al.* demonstrated almost single molecule level detection of DNA by electrochemical, voltametric sensors based on vertically oriented graphene nanowalls [93]. Vertically grown graphene provides extraordinary access to edge plane defects and allowing more efficient heterogeneous electron exchange and this leads to better electrochemical sensitivity. Araque *et al.* further improved the performance of textured 2D material based electrochemical sensors by employing 3D graphene as a nanoscale conductive scaffold to avoid aggregation of nanoparticles and showed robust, high sensitivity enzyme biosensing [94].

The works described above utilized graphene directly synthesized in a 3D format, limiting enhancement effects to increased surface area and modified access to edge sites. In reality, nanoscale mechanics driven crumpling of graphene offers even broader opportunities to increase sensitivity through heterogeneous chemical and physical modulation of graphene properties as discussed in the previous sections on texture mediated modulation of the wetting and EDL of 2D materials. Hwang *et al.* [57] recently reported crumpled graphene FETs (Fig. 9a-b) as electrical biosensors with substantial sensitivity enhancement, originating from EDL capacitance modulation and energy band gap opening of the crumpled graphene (Fig. 9c). Nanoscale crumples of graphene perturb EDL in ionic solutions and result in a decrease of capacitance

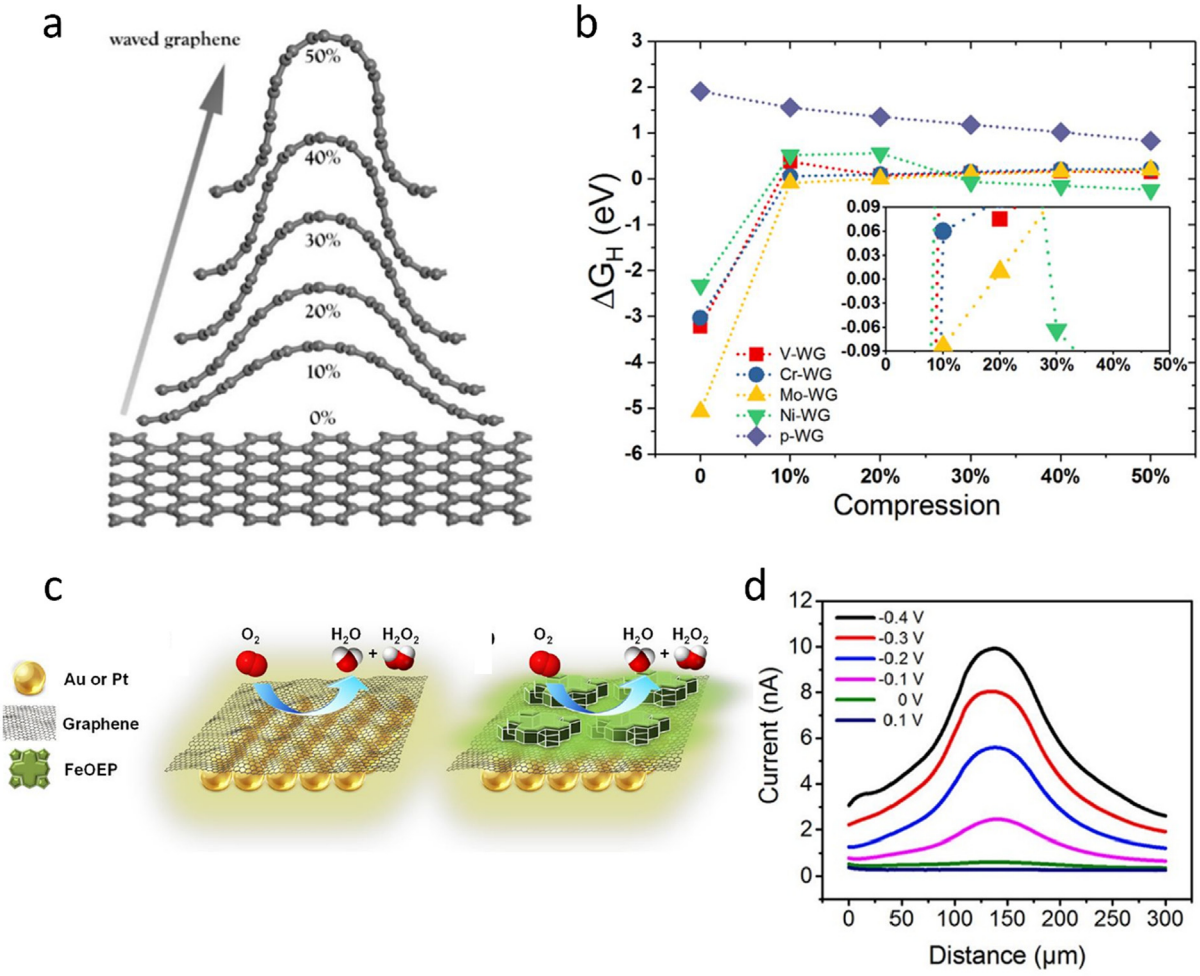

Fig. 8. (**a**) Illustration of wave-graphene with compression ratios from 0 to 50%. (**b**) Calculated overpotentials of V-, Cr-, Mo- and Ni-WG as a function of compression ratios from 0 to 50%. [Reprinted (adapted) with permission from Ref. [74]. Copyright (2018) American Chemical Society.]. (**c**) Heterostructured electrocatalysts separated by electrically "semi-transparent" graphene which allows the metal underlayer to affect ORR activity above graphene. (**d**) Lateral scans over the graphene/gold particle with substrate bias ranging from −0.4 to 0.1, increased current indicates enhanced ORR [Reprinted (adapted) with permission from Ref. [75]. Copyright (2018) American Chemical Society.]

values due to reduced Debye screening effect. Reduced Debye screening effect in this region allows higher detection sensitivity. Furthermore, computational simulations confirm that strain from the crumpling can open the energy bandgap of graphene, significantly increasing sensitivity to charged molecules (Fig. 9d). Demonstrated crumpled graphene FETs possessed extremely low LOD of 600 zM in 50 μL, where ~18 molecules were detectable in an hour on a millimeter sized device, which is more than 10,000 times enhancement than previous reports in graphene FET biosensing (Fig. 9e–f). None of the previous works using electrical or electrochemical platforms were able to detect nucleic acids below aM concentration level, especially with millimeter-sized devices within a 1 h timescale. Considering the incubation time and diffusion time estimated by Hwang *et al.*, it is possibly only 16% of the target molecules would be bound on the graphene surface. If that is the case, this platform can detect 2–3 DNA molecules, indicating the feasibility of single biomolecule detection [57].

In contrast to biomolecule sensing which relies on chemical binding, activity of complicated biosystems such as cells can be monitored via detection of electrical action potentials originating from neurons or muscle cells. An action potential is a rapid rise and subsequent fall in voltage or membrane potential across a cellular membrane and has a characteristic pattern that can be read by an external electrical device. Early studies showed cell activity monitoring using 1D and 2D materials. Cohen-Karni *et al.* demonstrated monitoring signals from embryonic chicken cardiomyocytes using both Si-nanowire and graphene FETs [95]. Li *et al.* used graphene FETs to record optogenetic cell activity [96]. However, as the minimum detectable signal of graphene transistor-based probes is inversely proportional to the square root of the active graphene area, higher surface-to-volume area would provide better monitoring. Yang *et al.* tried to address the limit of 2D graphene using crumpled transistors formed by compressing flat graphene down to 16% of its initial area [97]. Similarly, Kim *et al.* demonstrated potential implantable muscle monitoring system using uniaxially crumpled graphene electrode [98].

In addition to enhancing sensitivity for biomolecules, texturing driven modification of 2D material properties can be used to direct cell growth. Adhesion, proliferation, and differentiation of various mammalian cells on 2D graphene and its derivatives have been extensively studied [99]. Lee *et al.* found that differentiation of human mesenchymal stem cells (hMSCs) was directed towards osteogenic lineage on graphene while hSMCs differentiated to adipogenic lineage on graphene oxide [100]. Furthermore, it was shown that graphene induced human neural stem cells differentiation into neurons rather than glial cells [101]. In addition, graphene showed great cytocompatibility so that purified neuron cells can survive without supporting glial layer or protein coating [102]. Graphene and graphene oxide showed opposite roles on differentiation of induced pluripotent stem cells into endodermal lineage [103].

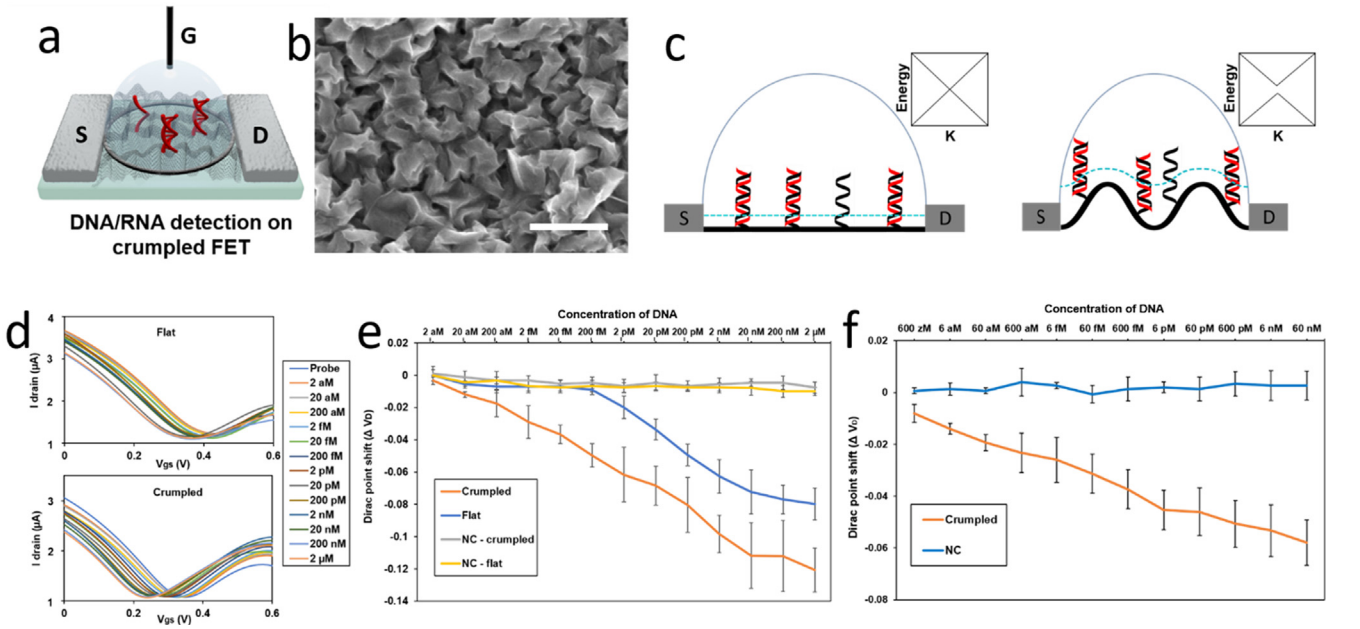

Fig. 9. Deformed graphene channel FET DNA sensor. (**a**) Graphene FET biosensor scheme where 'S' is source, 'D' is drain and 'G' is liquid gate electrode. (**b**) SEM images of crumpled graphene (500 nm scale bar). (**c**) Cross-section of the flat (left) and crumpled (right) graphene FET DNA sensor s. Probe (black) DNA strands are immobilized on the surface of graphene and target (red) strands were bound with it. Blue dotted correspond to the Debye length in the ionic solution, length is increased on concave regions of crumpled graphene allowing more DNA area inside the Debye length, increasing electrical susceptibility to negatively charged DNA. Inset boxes correspond to qualitative energy diagrams in K-space, while graphene does not have intrinsic bandgap, crumpling may open a bandgap. (**d**) I-V relationship for flat (top) and crumpled (bottom) graphene FET sensors with hybridized DNA. The DNA hybridization driven shifted of the I-V curve correlated to the concentration of DNA in solution. The I-V curve shifts on crumpled graphene is significantly larger than the IV- curve shift on flat graphene. (**e**) Dirac voltage shift with hybridization of DNA probes on FET sensors. NC refers to response to non-complementary control DNA sequences. (**f**) Dirac voltage shift with hybridization of PNA probes on FET sensors with. All data points are obtained from three devices. mean ± std. *P < 0.05. [Modified after (Hwang et al.) [57]. (© 2020, SpringerNature) (license: https://creativecommons.org/licenses/by/4.0/legalcode)]. (For interpretation of the references to color in this figure legend, the reader is referred to the web version of this article.)

As 2D graphene is an ideal material for micro- or nano-patterning or fabrication, it has been broadly employed to guide cellular assembly [98]. Wang *et al.* showed alignment of fibroblasts on uniaxially crumpled graphene, when C2C12 mouse myoblast cells were seeded on their platform. Kim *et al.* further demonstrated that wavy graphene surfaces (Fig. 10a–b) not only induce the alignment and elongation at a single-cell level but also enhance differentiation and maturation of myotubes compared to cells on flat graphene (Fig. 10c–d) [98,104,105]. Owing to the ease of fabrication and scalability, the crumpled graphene cellular template can be promising tool for tissue engineering and regenerative medicine for skeletal muscle tissues.

Employing 3D textured graphene in bio-applications is still in its early stages. So far, in most cases 3D textured graphene was used for increasing the surface-to-volume ratio. A few recent works have shown that interesting physical and chemical phenomena at near the nano-scale curvature of the 2D material enhance sensing and it is anticipated that more research will focus on expanding this concept. To date, crumpled graphene FET-based biosensors have only shown nucleic acid detection so it will be of interest to see if other biomarkers also can be detectable by crumpled graphene FETs with superior sensitivity and selectivity. Furthermore, Hwang *et al.* only showed biomolecular detection on macro-scale devices, therefore miniaturization of the device in arrayed format should allow even better sensitivity, high throughput, and parallel detection of many biomarkers [57]. Moreover, a few works have shown that the usefulness of crumpled graphene as scaffolds for templating of neurons and muscular cells. Therefore, other kinds of cells and cell mixtures such as neuro-muscular junction can be tested on the crumpled graphene in the future. Also, cellular templating with different crumpling geometries can be researched to study more active interface between deformed 2D materials and biosystem. Graphene is known to be flexible and stretchable however, deformed 2D materials can provide much better functionality on these features. As graphene is biocompatible and non-toxic material, it can be expected that crumpled graphene can be useful in bio-applications such as flexible, wearable, implantable and skin electronics.

7. Conclusion

In conclusion, while it is understood that 3D structures modulate wettability and electrostatic interaction at the solid liquid interface, the study of 3D texturing on 2D material-liquid interaction has been limited. Given the complex, heterogeneous effect of texturing on 2D materials' surface properties, crumpling 2D materials could serve as a unique route to tune fluid interaction. Texture enabled heterogeneous chemical modification of 2D materials may influence the local contact state of liquids with 2D materials. Similarly, texturing 2D materials could have the combined effect of directly obstructing liquid slippage while creating a corrugated energy landscape resulting in frictional behavior which varies between polar and non-polar solvents. Finally, heterogeneous band structure modulation and extrinsic doping effects of texturing could further result in complex modulation of wetting over a textured 2D material surface. Unfortunately, previous work on 3D textured 2D material fluid interaction has been limited to observation of a transition in water contact from Wentzel to Cassie Baxter states and basic simulation of fluid interaction in systems which resemble 3D textures including carbon nanotubes and graphene bilayers. In order to broaden current understanding of liquid – textured 2D material fluid interaction, it is necessary to develop methods to inform continuum scale simulations with inputs of small volume atomistic simulations at local points which can be combined with experimental local probing of surface properties with macroscale contact angle and flow measurement. Sophisticated understanding of the influencing of texturing on 2D

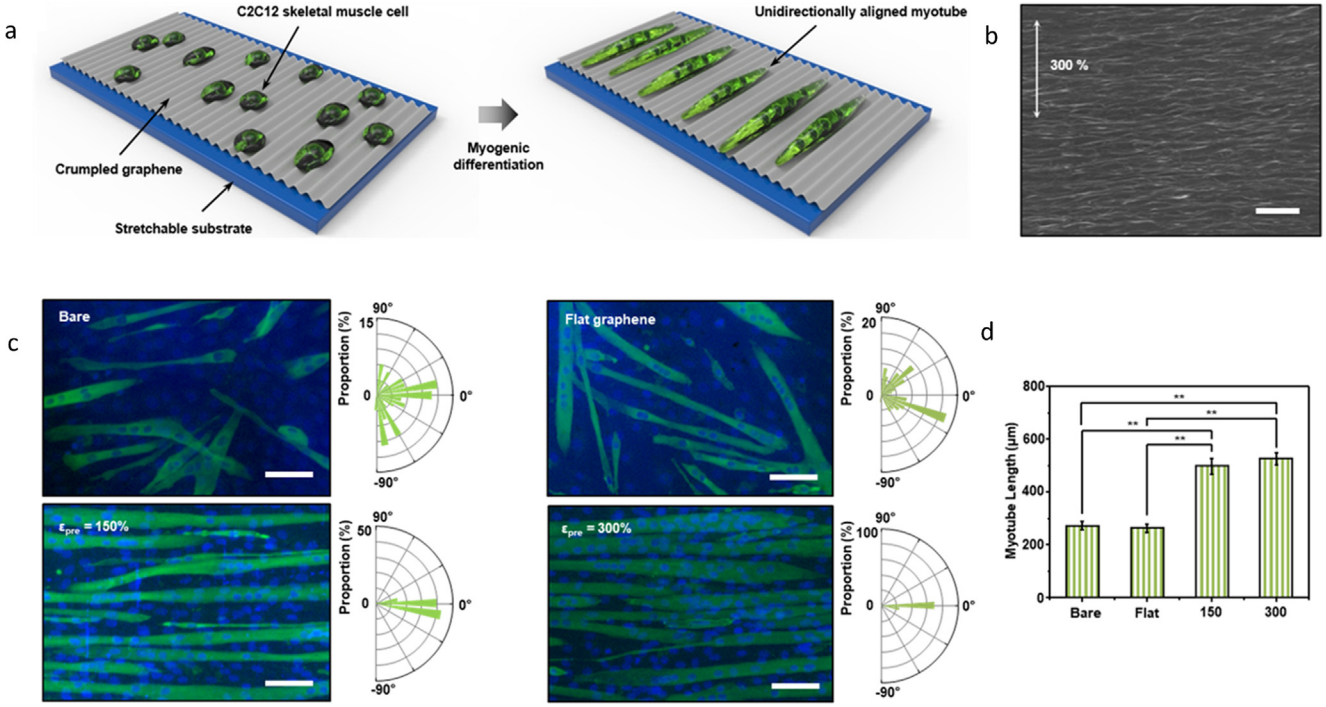

Fig. 10. Myotube differentiation on uniaxially crumpled graphene. (**a**) Myogenic differentiation and alignment of C2C12 cells on crumpled graphene (**b**) SEM images of crumpled graphene fabricated using a 300% pre-strain (scale bar equal: 1 μm). (**c**) Fluorescence images and angular distribution of myotubes on crumpled graphene with different surface conditions. Images were taken after 7 days of C2C12 differentiation in differential media, to gauge alignment and differentiation, myotubes and nuclei were stained for anti-myosin heavy chain (green) and DAPI (blue), respectively (scale bar equals 100 μm). (**d**) Quantification of myotube length. Significance: ** $p < 0.01$ and * $p < 0.05$. Data represented as the mean ± standard error ($n = 5$, in the case of the myotube aspect ratio, $n = 100$)[Modified after (Kim et al.) [105]. (© 2019, SpringerNature) (license: https://creativecommons.org/licenses/by/4.0/legalcode)]. (For interpretation of the references to color in this figure legend, the reader is referred to the web version of this article.)

material liquid interaction will permit diverse application including chemical barriers, friction-controlled surfaces and complex structures for energy storage, sensing, catalysis, and templating.

Recent theoretical explorations, using atomistic MD simulation, have begun to elucidate the specific interaction of molecules dispersed in an aqueous phase with textured 2D materials. It is now known that the structural properties of the EDL next to textured and flat graphene differ considerably. Most importantly, near concave sections of a textured graphene surface ions are confined to a higher degree increasing the thickness of the EDL. This increased EDL thickness results in a reduction in molecular screening which could lead to the development of highly sensitive chemical sensors. Furthermore, modified ionic interaction enabled by texturing has shown promise for improving the performance of EDL capacitors by increasing the quantum capacitance of the 2D materials used in their construction and increased the number of entrained ions. Lastly, texture driven variation in surface chemistry extends tuning beyond ionic interaction enabling a variety of options for tuning fluid phase chemistry including amplification of the HER and the ORR over graphene surfaces.

Modified fluid structure and chemical interaction near textured 2D material surfaces has informed the development of advanced systems for sensing biomolecules and templating cellular growth. Crumpled graphene FETs used as a biosensor demonstrated gigantic sensitivity enhancement. EDL capacitance change and energy band gap opening enabled by crumpling graphene resulted in a 10,000 times enhancement in sensitivity compared to flat graphene FET biosensors. At the reported sensitivity level crumpled graphene FET platforms offer the possibility of single biomolecule detection. Moreover, crumpled graphene based sensors have shown promise for monitoring biological networks including individual cells and cell ensembles by detecting action potentials in cultured neuron and muscle tissue. Crumpled graphene shows the greatest utility in guiding cellular assembly with wavy textured graphene promoting alignment, differentiation, and maturation of myotubes cultures across the crumpled graphene surface. Continuing study of the effects of 3D texturing on 2D material fluid interaction and expanding studies to include newly developed 2D materials and diverse texturing geometries will enable even greater opportunities for tuning fluid phase interaction to develop advanced surfaces, sensors, energy storage systems, and biological templates.

Declaration of Competing Interest

The authors declare that they have no known competing financial interests or personal relationships that could have appeared to influence the work reported in this paper.

Acknowledgements

We gratefully acknowledge support from the National Science Foundation (MRSEC DMR-1720633 and DMR-1708852) and Defense Threat Reduction Agency (HDTRA1620298). P.S. gratefully acknowledges support from the NASA Space Technology Research Fellowship (NNX16AM69H). This work was primarily supported by the NSF through the University of Illinois at Urbana-Champaign Materials Research Science and Engineering Center DMR-1720633.

Declaration of Competing Interest

The authors declared that there is no conflict of interest.

References

[1] A.K. Geim, Graphene: Status and Prospects, Science 324 (5934) (2009) 1530–1534 https://www.sciencemag.org/lookup/doi/10.1126/science:1158877https://doi.

org/10.1126/science:1158877.
[2] M.R.E. Tanjil, Y. Jeong, Z. Yin, W. Panaccione, M.C. Wang, Ångström-scale, atomically thin 2D materials for corrosion mitigation and passivation, Coatings. 9 (2019) 133.
[3] K.S. Novoselov, A.K. Geim, S.V. Morozov, D. Jiang, M.I. Katsnelson, I.V. Grigorieva, S.V. Dubonos, A.A. Firsov, Two-dimensional gas of massless Dirac fermions in graphene, Nature. 438 (2005) 197–200.
[4] X. Wang, G. Shi, An introduction to the chemistry of graphene, Phys. Chem. Chem. Phys. 17 (2015) 28484–28504.
[5] P. Snapp, J.M. Kim, C. Cho, J. Leem, M.F. Haque, S. Nam, Interaction of 2D materials with liquids: wettability, electrochemical properties, friction, and emerging directions, NPG Asia Mater. 12 (2020) 1–16.
[6] D. Parobek, H. Liu, Wettability of graphene, 2D Mater. 2 (2015) 032001.
[7] Y. Wu, N.R. Aluru, Graphitic carbon-water nonbonded interaction parameters, J. Phys. Chem. B. 117 (2013) 8802–8813.
[8] M. Annamalai, K. Gopinadhan, S.A. Han, S. Saha, H.J. Park, E.B. Cho, B. Kumar, A. Patra, S.W. Kim, T. Venkatesan, Surface energy and wettability of van der Waals structures, Nanoscale. 8 (2016) 5764–5770.
[9] A.I. Aria, P.R. Kidambi, R.S. Weatherup, L. Xiao, J.A. Williams, S. Hofmann, Time Evolution of the Wettability of Supported Graphene under Ambient Air Exposure, J. Phys. Chem. C. 120 (2016) 2215–2224.
[10] S.S. Kwon, J. Choi, M. Heiranian, Y. Kim, W.J. Chang, P.M. Knapp, M.C. Wang, J.M. Kim, N.R. Aluru, W. Il Park, S.W. Nam, Electrical Double Layer of Supported Atomically Thin Materials, Nano Lett. 19 (2019) 4588–4593.
[11] M.C. Wang, J. Leem, P. Kang, J. Choi, P. Knapp, K. Yong, S.W. Nam, Mechanical instability driven self-assembly and architecturing of 2D materials, 2D, Mater. 4 (2017) 022002.
[12] H. Qin, Y. Sun, J.Z. Liu, Y. Liu, Mechanical properties of wrinkled graphene generated by topological defects, Carbon N. Y. 108 (2016) 204–214.
[13] P. Kang, M.C. Wang, P.M. Knapp, S.W. Nam, Crumpled Graphene Photodetector with Enhanced, Strain-Tunable, and Wavelength-Selective Photoresponsivity, Adv. Mater. 28 (2016) 4639–4565.
[14] B. Ouyang, P. Ou, J. Song, Controllable Phase Stabilities in Transition Metal Dichalcogenides through Curvature Engineering: First-Principles Calculations and Continuum Prediction, Adv. Theory Simul. 1 (2018) 1800003.
[15] W.K. Lee, W. Bin Jung, S.R. Nagel, T.W. Odom, Stretchable superhydrophobicity from monolithic, three-dimensional hierarchical wrinkles, Nano Lett. 16 (2016) 3774–3779.
[16] K. Shoorideh, C.O. Chui, On the origin of enhanced sensitivity in nanoscale FET-based biosensors, Proc. Natl. Acad. Sci. U. S. A. 111 (2014) 5111–5116.
[17] J. Zang, S. Ryu, N. Pugno, Q. Wang, Q. Tu, M.J. Buehler, X. Zhao, Multifunctionality and control of the crumpling and unfolding of large-area graphene, Nat. Mater. 12 (2013) 321–325.
[18] S. Deng, D. Rhee, W.K. Lee, S. Che, B. Keisham, V. Berry, T.W. Odom, Graphene Wrinkles Enable Spatially Defined Chemistry, Nano Lett. 19 (2019) 5640–5646.
[19] Y. Diao, G. Greenwood, M.C. Wang, S. Nam, R.M. Espinosa-Marzal, Slippery and sticky graphene in water, ACS Nano. 13 (2019) 2072–2082.
[20] A. Ashraf, Y. Wu, M.C. Wang, K. Yong, T. Sun, Y. Jing, R.T. Haasch, N.R. Aluru, S. Nam, Doping-induced tunable wettability and adhesion of graphene, Nano Lett. 16 (2016) 4708–4712.
[21] Z. Pan, N. Liu, L. Fu, Z. Liu, Wrinkle engineering: A new approach to massive graphene nanoribbon arrays, J. Am. Chem. Soc. 133 (2011) 17578–17581.
[22] Y. Zhang, M. Heiranian, B. Janicek, Z. Budrikis, S. Zapperi, P.Y. Huang, H.T. Johnson, N.R. Aluru, J.W. Lyding, N. Mason, Strain Modulation of Graphene by Nanoscale Substrate Curvatures: A Molecular View, Nano Lett. 18 (2018) 2098–2104.
[23] W.K. Lee, J. Kang, K.S. Chen, C.J. Engel, W. Bin Jung, D. Rhee, M.C. Hersam, T.W. Odom, Multiscale, Hierarchical Patterning of Graphene by Conformal Wrinkling, Nano Lett. 16 (2016) 7121–7127.
[24] M.C. Wang, S. Chun, R.S. Han, A. Ashraf, P. Kang, S. Nam, Heterogeneous, three-dimensional texturing of graphene, Nano Lett. 15 (2015) 1829–1835.
[25] P.Y. Chen, J. Sodhi, Y. Qiu, T.M. Valentin, R.S. Steinberg, Z. Wang, R.H. Hurt, I.Y. Wong, Multiscale Graphene Topographies Programmed by Sequential Mechanical Deformation, Adv. Mater. 28 (2016) 3564–3571.
[26] J. Choi, H.J. Kim, M.C. Wang, J. Leem, W.P. King, S. Nam, Three-Dimensional Integration of Graphene via Swelling, Shrinking, and Adaptation, Nano Lett. 15 (2015) 4525–4531.
[27] J. Choi, J. Mun, M.C. Wang, A. Ashraf, S.W. Kang, S.W. Nam, Hierarchical, Dual-Scale Structures of Atomically Thin MoS 2 for Tunable Wetting, Nano Lett. 17 (2017) 1756–1761.
[28] J. Feng, Z. Guo, Wettability of graphene: From influencing factors and reversible conversions to potential applications, Nanosc. Horiz. 4 (2019) 526–530.
[29] S. Deng, A.V. Sumant, V. Berry, Strain engineering in two-dimensional nanomaterials beyond graphene, Nano Today. 22 (2018) 14–35.
[30] A. Ashraf, Y. Wu, M.C. Wang, N.R. Aluru, S.A. Dastgheib, S.W. Nam, Spectroscopic investigation of the wettability of multilayer graphene using highly ordered pyrolytic graphite as a model material, Langmuir. 30 (2014) 12827–12836.
[31] J. Son, N. Buzov, S. Chen, D. Sung, H. Ryu, J. Kwon, S.P. Kim, S. Namiki, J. Xu, S. Hong, K. Watanabe, T. Taniguchi, W.P. King, G.H. Lee, A.M. van der Zande, Tailoring Surface Properties via Functionalized Hydrofluorinated Graphene Compounds, Adv. Mater. 31 (2019) 1903424.
[32] P. Zhu, R. Li, Study of Nanoscale Friction Behaviors of Graphene on Gold Substrates Using Molecular Dynamics, Nanoscale Res. Lett. 13 (2018) 1–8.
[33] R. Shi, L. Gao, H. Lu, Q. Li, T.B. Ma, H. Guo, S. Du, X.Q. Feng, S. Zhang, Y. Liu, P. Cheng, Y.Z. Hu, H.J. Gao, J. Luo, Moiré superlattice-level stick-slip instability originated from geometrically corrugated graphene on a strongly interacting substrate, 2D, Mater. 4 (2017) 025079.
[34] G. Tocci, L. Joly, A. Michaelides, Friction of water on graphene and hexagonal boron nitride from Ab initio methods: Very different slippage despite very similar interface structures, Nano Lett. 14 (2014) 6872–6877.
[35] A. Govind Rajan, M.S. Strano, D. Blankschtein, Liquids with Lower Wettability Can Exhibit Higher Friction on Hexagonal Boron Nitride: The Intriguing Role of Solid-Liquid Electrostatic Interactions, Nano Lett. 19 (2019) 1539–1551.
[36] J. Wang, R. Zhao, M. Yang, Z. Liu, Z. Liu, Inverse relationship between carrier mobility and bandgap in graphene, J. Chem. Phys. 138 (2013) 084701.
[37] X. Peng, F. Tang, A. Copple, Engineering the work function of armchair graphene nanoribbons using strain and functional species: A first principles study, J. Phys. Condens. Matter. 24 (2012) 075501.
[38] M.A. Bissett, S. Konabe, S. Okada, M. Tsuji, H. Ago, Enhanced chemical reactivity of graphene induced by mechanical strain, ACS Nano. 7 (2013) 10335–10343.
[39] J. Pu, S. Wan, Z. Lu, G.A. Zhang, L. Wang, X. Zhang, Q. Xue, Controlled water adhesion and electrowetting of conducting hydrophobic graphene/carbon nanotubes composite films on engineering materials, J. Mater. Chem. A. 1 (2013) 1254–1260.
[40] J.A. Thomas, A.J.H. McGaughey, Density, distribution, and orientation of water molecules inside and outside carbon nanotubes, J. Chem. Phys. 128 (2008) 084715.
[41] N. Patra, D.A. Esan, P. Král, Dynamics of ion binding to graphene nanostructures, J. Phys. Chem. C. 117 (2013) 10750–10754.
[42] Graphene Field Effect Transistors for Biomedical Applications, Current Status and Future Prospects, Diagnostics. 7 (2017) 45.
[43] B.J. Kim, S.K. Lee, M.S. Kang, J.H. Ahn, J.H. Cho, Coplanar-gate transparent graphene transistors and inverters on plastic, ACS Nano. 6 (2012) 8646–8651.
[44] D. Sarkar, W. Liu, X. Xie, A.C. Anselmo, S. Mitragotri, K. Banerjee, MoS2 field-effect transistor for next-generation label-free biosensors, ACS Nano. 8 (2014) 3992–4003.
[45] T. Fujimoto, K. Awaga, Electric-double-layer field-effect transistors with ionic liquids, Phys. Chem. Chem. Phys. 15 (2013) 8983–9006.
[46] G.S. Kulkarni, Z. Zhong, Detection beyond the Debye screening length in a high-frequency nanoelectronic biosensor, Nano Lett. 12 (2012) 719–723.
[47] E. Stern, R. Wagner, F.J. Sigworth, R. Breaker, T.M. Fahmy, M.A. Reed, Importance of the debye screening length on nanowire field effect transistor sensors, Nano Lett. 7 (2007) 3405–3409.
[48] M. Kaisti, Detection principles of biological and chemical FET sensors, Biosens. Bioelectron. 98 (2017) 437–448.
[49] G. Zheng, F. Patolsky, Y. Cui, W.U. Wang, C.M. Lieber, Multiplexed electrical detection of cancer markers with nanowire sensor arrays, Nat. Biotechnol. 23 (2005) 1294–1301.
[50] E. Stern, A. Vacic, N.K. Rajan, J.M. Criscione, J. Park, B.R. Ilic, D.J. Mooney, M.A. Reed, T.M. Fahmy, Label-free biomarker detection from whole blood, Nat. Nanotechnol. 5 (2010) 138–142.
[51] N. Gao, W. Zhou, X. Jiang, G. Hong, T.M. Fu, C.M. Lieber, General strategy for biodetection in high ionic strength solutions using transistor-based nanoelectronic sensors, Nano Lett. 15 (2015) 2143–2148.
[52] A. Susloparova, D. Koppenhöfer, J.K.Y. Law, X.T. Vu, S. Ingebrandt, Electrical cell-substrate impedance sensing with field-effect transistors is able to unravel cellular adhesion and detachment processes on a single cell level, Lab Chip. 15 (2015) 668–679.
[53] S. Schäfer, S. Eick, B. Hofmann, T. Dufaux, R. Stockmann, G. Wrobel, A. Offenhäusser, S. Ingebrandt, Time-dependent observation of individual cellular binding events to field-effect transistors, Biosens. Bioelectron. 24 (2009) 1201–1208.
[54] S. Ingebrandt, Y. Han, F. Nakamura, A. Poghossian, M.J. Schöning, A. Offenhäusser, Label-free detection of single nucleotide polymorphisms utilizing the differential transfer function of field-effect transistors, Biosens. Bioelectron. 22 (2007) 2834–2840.
[55] K. Maehashi, T. Katsura, K. Kerman, Y. Takamura, K. Matsumoto, E. Tamiya, Label-free protein biosensor based on aptamer-modified carbon nanotube field-effect transistors, Anal. Chem. 79 (2007) 782–787.
[56] R. Elnathan, M. Kwiat, A. Pevzner, Y. Engel, L. Burstein, A. Khatchtourints, A. Lichtenstein, R. Kantaev, F. Patolsky, Biorecognition layer engineering: Overcoming screening limitations of nanowire-based FET devices, Nano Lett. 12 (2012) 5245–5254.
[57] M.T. Hwang, M. Heiranian, Y. Kim, S. You, J. Leem, A. Taqieddin, V. Faramarzi, Y. Jing, I. Park, A.M. van der Zande, S. Nam, N.R. Aluru, R. Bashir, Ultrasensitive detection of nucleic acids using deformed graphene channel field effect biosensors, Nat. Commun. 11 (2020) 1–11.
[58] P. Simon, Y. Gogotsi, Materials for electrochemical capacitors, Nat. Mater. 7 (2008) 845–854.
[59] Y. Gogotsi, A. Nikitin, H. Ye, W. Zhou, J.E. Fischer, B. Yi, H.C. Foley, M.W. Barsoum, Nanoporous carbide-derived carbon with tunable pore size, Nat. Mater. 2 (2003) 591–594.
[60] L.L. Zhang, X.S. Zhao, Carbon-based materials as supercapacitor electrodes, Chem. Soc. Rev. 38 (2009) 2520–2531.
[61] Y. Zhai, Y. Dou, D. Zhao, P.F. Fulvio, R.T. Mayes, S. Dai, Carbon Materials for Chemical Capacitive Energy Storage, Adv. Mater. 23 (2011) 4828–4850.
[62] M.D. Stoller, C.W. Magnuson, Y. Zhu, S. Murali, J.W. Suk, R. Piner, R.S. Ruoff, Interfacial capacitance of single layer graphene, Energy Environ. Sci. 4 (2011) 4685–4689.
[63] E. Paek, A.J. Pak, G.S. Hwang, A computational study of the interfacial structure and capacitance of graphene in [BMIM][PF6] ionic liquid, J. Electrochem. Soc. 160 (2013) A1–A10.

[64] H. Ji, X. Zhao, Z. Qiao, J. Jung, Y. Zhu, Y. Lu, L.L. Zhang, A.H. MacDonald, R.S. Ruoff, Capacitance of carbon-based electrical double-layer capacitors, Nat. Commun. 5 (2014) 3317.

[65] C. Zhan, J. Neal, J. Wu, D.E. Jiang, Quantum Effects on the Capacitance of Graphene-Based Electrodes, J. Phys. Chem. C. 119 (2015) 22297–22303.

[66] C. Zhan, Y. Zhang, P.T. Cummings, D.E. Jiang, Enhancing graphene capacitance by nitrogen: Effects of doping configuration and concentration, Phys. Chem. Chem. Phys. 18 (2016) 4668–4674.

[67] J. Chen, Y. Han, X. Kong, X. Deng, H.J. Park, Y. Guo, S. Jin, Z. Qi, Z. Lee, Z. Qiao, R.S. Ruoff, H. Ji, The Origin of Improved Electrical Double-Layer Capacitance by Inclusion of Topological Defects and Dopants in Graphene for Supercapacitors, Angew. Chemie - Int. Ed. 55 (2016) 13822–13827.

[68] M. Zeiger, D. Weingarth, V. Presser, Quinone-Decorated Onion-Like Carbon/Carbon Fiber Hybrid Electrodes for High-Rate Supercapacitor Applications, ChemElectroChem. 2 (2015) 1117–1127.

[69] M. Boota, C. Chen, M. Bécuwe, L. Miao, Y. Gogotsi, Pseudocapacitance and excellent cyclability of 2,5-dimethoxy-1,4-benzoquinone on graphene, Energy Environ. Sci. 9 (2016) 2586–2594.

[70] L.L. Zhang, X. Zhao, H. Ji, M.D. Stoller, L. Lai, S. Murali, S. McDonnell, B. Cleveger, R.M. Wallace, R.S. Ruoff, Nitrogen doping of graphene and its effect on quantum capacitance, and a new insight on the enhanced capacitance of N-doped carbon, Energy Environ. Sci. 5 (2012) 9618–9625.

[71] B.C. Wood, T. Ogitsu, M. Otani, J. Biener, First-principles-inspired design strategies for graphene-based supercapacitor electrodes, J. Phys. Chem. C. 118 (2014) 4–15.

[72] C. Zhan, T.A. Pham, M.R. Cerón, P.G. Campbell, V. Vedharathinam, M. Otani, D.E. Jiang, J. Biener, B.C. Wood, M. Biener, Origins and Implications of Interfacial Capacitance Enhancements in C 60 -Modified Graphene Supercapacitors, ACS Appl. Mater. Interfaces. 10 (2018) 36860–36865.

[73] L.M. Xie, Two-dimensional transition metal dichalcogenide alloys: Preparation, characterization and applications, Nanoscale. 7 (2015) 18392–18401.

[74] Y. Qu, Y. Ke, Y. Shao, W. Chen, C.T. Kwok, X. Shi, H. Pan, Effect of Curvature on the Hydrogen Evolution Reaction of Graphene, J. Phys. Chem. C. 122 (2018) 25331–25338.

[75] J. Hui, S. Pakhira, R. Bhargava, Z.J. Barton, X. Zhou, A.J. Chinderle, J.L. Mendoza-Cortes, J. Rodríguez-López, Modulating Electrocatalysis on Graphene Heterostructures: Physically Impermeable Yet Electronically Transparent Electrodes, ACS Nano. 12 (2018) 2980–2990.

[76] J. Son, S. Lee, S.J. Kim, B.C. Park, H.K. Lee, S. Kim, J.H. Kim, B.H. Hong, J. Hong, Hydrogenated monolayer graphene with reversible and tunable wide band gap and its field-effect transistor, Nat. Commun. 7 (2016) 13261.

[77] L. Yan, Y.B. Zheng, F. Zhao, S. Li, X. Gao, B. Xu, P.S. Weiss, Y. Zhao, Chemistry and physics of a single atomic layer: Strategies and challenges for functionalization of graphene and graphene-based materials, Chem. Soc. Rev. 41 (2012) 97–114.

[78] Q. Wu, Y. Wu, Y. Hao, J. Geng, M. Charlton, S. Chen, Y. Ren, H. Ji, H. Li, D.W. Boukhvalov, R.D. Piner, C.W. Bielawski, R.S. Ruoff, Selective surface functionalization at regions of high local curvature in graphene, Chem. Commun. 49 (2012) 677–679.

[79] J.T. Rasmussen, T. Gunst, P. Bøggild, A.P. Jauho, M. Brandbyge, Electronic and transport properties of kinked graphene, Beilstein J. Nanotechnol. 4 (2013) 103–110.

[80] A. Ganguli, Y. Watanabe, M.T. Hwang, J.C. Huang, R. Bashir, Robust label-free microRNA detection using one million ISFET array, Biomed. Microdevices. 20 (2018) 45.

[81] J.W. Ko, J.M. Woo, A. Jinhong, J.H. Cheon, J.H. Lim, S.H. Kim, H. Chun, E. Kim, Y.J. Park, Multi-order dynamic range DNA sensor using a gold decorated SWCNT random network, ACS Nano. 5 (2011) 4365–4372.

[82] A. Gao, N. Lu, P. Dai, T. Li, H. Pei, X. Gao, Y. Gong, Y. Wang, C. Fan, Silicon-nanowire-based CMOS-compatible field-effect transistor nanosensors for ultra-sensitive electrical detection of nucleic acids, Nano Lett. 11 (2011) 3974–3978.

[83] Y. Huang, X. Dong, Y. Shi, C.M. Li, L.J. Li, P. Chen, Nanoelectronic biosensors based on CVD grown graphene, Nanoscale. 2 (2010) 1485–1488.

[84] N. Mohanty, V. Berry, Graphene-based single-bacterium resolution biodevice and DNA transistor: Interfacing graphene derivatives with nanoscale and microscale biocomponents, Nano Lett. 8 (2008) 4469–4476.

[85] Y.H. Kwak, D.S. Choi, Y.N. Kim, H. Kim, D.H. Yoon, S.S. Ahn, J.W. Yang, W.S. Yang, S. Seo, Flexible glucose sensor using CVD-grown graphene-based field effect transistor, Biosens. Bioelectron. 37 (2012) 82–87.

[86] N.S. Green, M.L. Norton, Interactions of DNA with graphene and sensing applications of graphene field-effect transistor devices: A review, Anal. Chim. Acta. 853 (2015) 127–142.

[87] Y. Ohno, K. Maehashi, Y. Yamashiro, K. Matsumoto, Electrolyte-gated graphene field-effect transistors for detecting ph and protein adsorption, Nano Lett. 9 (2009) 3318–3322.

[88] M.T. Hwang, P.B. Landon, J. Lee, D. Choi, A.H. Mo, G. Glinsky, R. Lal, Highly specific SNP detection using 2D graphene electronics and DNA strand displacement, Proc. Natl. Acad. Sci. U. S. A. 113 (2016) 7088–7093.

[89] M.T. Hwang, Z. Wang, J. Ping, D.K. Ban, Z.C. Shiah, L. Antonschmidt, J. Lee, Y. Liu, A.G. Karkisaval, A.T.C. Johnson, C. Fan, G. Glinsky, R. Lal, DNA nanotweezers and graphene transistor enable label-free genotyping, Adv. Mater. 30 (2018) 1802440.

[90] N.M. Andoy, M.S. Filipiak, D. Vetter, Ó. Gutiérrez-Sanz, A. Tarasov, Graphene-Based Electronic Immunosensor with Femtomolar Detection Limit in Whole Serum, Adv. Mater. Technol. 3 (2018) 1800186.

[91] G. Xu, J. Abbott, L. Qin, K.Y.M. Yeung, Y. Song, H. Yoon, J. Kong, D. Ham, Electrophoretic and field-effect graphene for all-electrical DNA array technology, Nat. Commun. 5 (2014) 4866.

[92] P. Kumar Roy, A. Ganguly, W.H. Yang, C.T. Wu, J.S. Hwang, Y. Tai, K.H. Chen, L.C. Chen, S. Chattopadhyay, Edge promoted ultrasensitive electrochemical detection of organic bio-molecules on epitaxial graphene nanowalls, Biosens. Bioelectron. 70 (2015) 137–144.

[93] O. Akhavan, E. Ghaderi, R. Rahighi, Toward single-DNA electrochemical biosensing by graphene nanowalls, ACS Nano. 6 (2012) 2904–2916.

[94] E. Araque, R. Villalonga, M. Gamella, P. Martínez-Ruiz, J. Reviejo, J.M. Pingarrón, Crumpled reduced graphene oxide-polyamidoamine dendrimer hybrid nanoparticles for the preparation of an electrochemical biosensor, J. Mater. Chem. B. 1 (2013) 2289–2296.

[95] T. Cohen-Karni, Q. Qing, Q. Li, Y. Fang, C.M. Lieber, Graphene and nanowire transistors for cellular interfaces and electrical recording, Nano Lett. 10 (2010) 1098–1102.

[96] G. Li, J. Yang, W. Yang, F. Wang, Y. Wang, W. Wang, L. Liu, Label-free multi-dimensional information acquisition from optogenetically engineered cells using a graphene transistor, Nanoscale. 10 (2018) 2285–2290.

[97] L. Yang, Y. Zhao, W. Xu, E. Shi, W. Wei, X. Li, A. Cao, Y. Cao, Y. Fang, Highly crumpled all-carbon transistors for brain activity recording, Nano Lett. 17 (2017) 71–77.

[98] S.J. Kim, K.W. Cho, H.R. Cho, L. Wang, S.Y. Park, S.E. Lee, T. Hyeon, N. Lu, S.H. Choi, D.H. Kim, Stretchable and Transparent Biointerface Using Cell-Sheet-Graphene Hybrid for Electrophysiology and Therapy of Skeletal Muscle, Adv. Funct. Mater. 26 (2016) 3207–3217.

[99] S.H. Ku, M. Lee, C.B. Park, Carbon-Based Nanomaterials for Tissue Engineering, Adv. Healthc. Mater. 2 (2013) 244–260.

[100] W.C. Lee, C.H.Y.X. Lim, H. Shi, L.A.L. Tang, Y. Wang, C.T. Lim, K.P. Loh, Origin of enhanced stem cell growth and differentiation on graphene and graphene oxide, ACS Nano. 5 (2011) 7334–7341.

[101] S.Y. Park, J. Park, S.H. Sim, M.G. Sung, K.S. Kim, B.H. Hong, S. Hong, Enhanced differentiation of human neural stem cells into neurons on graphene, Adv. Mater. 23 (2011) H263–H267.

[102] A. Bendali, L.H. Hess, M. Seifert, V. Forster, A.F. Stephan, J.A. Garrido, S. Picaud, Purified Neurons can Survive on Peptide-Free Graphene Layers, Adv. Healthc. Mater. 2 (2013) 929–933.

[103] G.Y. Chen, D.W.P. Pang, S.M. Hwang, H.Y. Tuan, Y.C. Hu, A graphene-based platform for induced pluripotent stem cells culture and differentiation, Biomaterials. 33 (2012) 418–427.

[104] Z. Wang, D. Tonderys, S.E. Leggett, E.K. Williams, M.T. Kiani, R. Spitz Steinberg, Y. Qiu, I.Y. Wong, R.H. Hurt, Wrinkled, wavelength-tunable graphene-based surface topographies for directing cell alignment and morphology, Carbon N. Y. 97 (2016) 14–24.

[105] J. Kim, J. Leem, H.N. Kim, P. Kang, J. Choi, M.F. Haque, D. Kang, S. Nam, Uniaxially crumpled graphene as a platform for guided myotube formation, Microsystems Nanoeng. 5 (2019) 53.